Tutors

Drs. Montserrat Iborra Urios i Javier Tejero Salvador
Departament d'Enginyeria Química i Química Analítica.

Grau en Enginyeria Química

UNIVERSITAT DE BARCELONA

Treball Final de Grau

A contribution to the study of kinetics of the transformation of fructose into butyl levulinate in aqueous media.

Irati Escuer Elizalde

June 2024

Als meus tutors, per tot l'ajut que m'han brindat durant aquest temps i la pàciencia i dedicació que han volcat en mi. A tots els companys que m'han acompanyat al llarg d'aquest camí i l'han fet més fàcil i agradable. Als meus pares, per demostrar-me de manera incansable la seva confiança en mi. I a tu, Toni, per ser el meu recolzament més gran.

Gràcies.

CONTENTS

SUMMARY

The climate crisis has forced to accelerate the research of greener solutions to those already established in industry. In this search, alkyl levulinates have stood out due to their physico-chemical properties and their low toxicity. These compounds have interesting applications in a variety of fields, but they mostly outstand as oxygenate additives for gasoline and diesel, improving their quality and reducing their pollution. Especially, it has generated a great deal of interest butyl levulinate, since it has demonstrated to improve cold flow properties, conductivity and lubricity, among other properties.

Butyl levulinate can be obtained through an esterification of levulinic acid with 1-butanol in liquid phase. However, due to the difficulty of purifying the acid, is being studied its obtention from hexoses. Particularly, from fructose, since it has demonstrated to be the optimum route.

The process of obtaining butyl levulinate from fructose consist of a reaction network, where the reactions are given in series-parallel and are the following:

· Fructose dehydrates and forms 5-hydroximetil furfural (HMF).

· HMF is rehydrated and are obtained levulinic and formic acids.

· In parallel, HMF reacts with 1-butanol and gives 5-hydroxibutyl furfural (HBF).

· Levulinic and formic acids react with 1-butanol and produce butyl levulinate (BL) and butyl formate (BF), respectively.

· By thermal degradation of fructose and catalytic reaction of HMF, there is the undesired formation of humins.

Despite being a field with numerous advances in the last times, most of them are limited on academic studies. Hence, the necessity of the search of kinetic models that describe the process, as a first step to design and optimize the process in industrial scale.

Keywords: Butyl levulinate, fructose, kinetic model, alkyl levulinates, kinetic constant.

RESUM

La crisi climàtica ha obligat a accelerar la recerca de solucions més verdes a les ja establertes a la indústria. En aquesta cerca han destacat els alquil levulinats gràcies a les seves propietats físico-químiques i la seva baixa toxicitat. Aquests compostos tenen aplicacions interessants en diversos camps, però majoritàriament destaquen com a additius oxigenats per a gasolina i dièsel, ja que milloren la seva qualitat i redueixen la seva contaminació. En particular, ha generat un gran interès el butil levulinat, ja que ha demostrat millorar les propietats del flux en fred, la conductivitat i la lubricitat, entre d'altres.

L'obtenció del butil levulinat es pot dur a terme a través d'una esterificació de l'àcid levulinic amb 1-butanol en fase líquida. Ara bé, degut a les dificultats que presenta la purificació d'aquest àcid, s'està estudiant la seva obtenció a partir de hexoses. Concretament a partir de la fructosa, ja que ha demostrat ser un camí més òptim.

El procés per obtenir butil levulinat a partir de la fructosa el conforma una xarxa de reaccions, les quals es donen en sèrie-paral·lel i són les següents:

· La fructosa és deshidrata i forma 5-hidroximetil furfural (HMF).

· L'HMF es rehidrata i s'obté àcid levulinic i àcid fòrmic.

· Paral·lelament, l'HMF reacciona amb 1-butanol i dona 5-hidroxibutil furfural (HBF).

· Els àcids levulinic i fòrmic reaccionen amb 1-butanol i produeixen butil levulinat i formiat de butil, respectivament.

· Per degradació tèrmica de la fructosa i reacció catalítica del HMF, es dona la formació no desitjada d'humins.

Tot i ser un camp on ha hagut diversos avanços en els últims temps, la majoria d'ells es limiten a estudis acadèmics. És per això que és tan necessària la cerca de models cinètics que descriguin el procés, per poder dissenyar-lo i optimitzar-lo a gran escala.

Paraules clau: Butil levulinat, fructosa, model cinètic, alquil levulinats, constant cinètica.

SUSTAINABLE DEVELOPMENT GOALS

The 17 sustainable development goals can be categorized into the five Ps, which are:

- People
- Planet
- Prosperity
- Peace
- Partnership

The study of the obtention of butyl levulinate generated particular interest when it demonstrated be a greener additive for gasoline and diesel, and that is due to its oxygenate nature as additive, which reduces the pollution produced. Also, the obtention of petroleum-based additives generates high concentrations of carbon dioxide and other greenhouse effect gases. On the other hand, fructose can be obtained from biomass, naturally present in our planet. So, not just the final product results to be less pollutant for the planet, but also the process to obtain them.

Having said that, this current work is completely related with “Planet”, which says that we must protect planet from degradation, including a sustainable consumption and production, so that the planet can cover the human needs of the present and future generations. This term goes hand in hand with “Prosperity”. Prosperity involves an economic, social and technological development, and must ensure the protection, or not destruction, of nature. This development pretends to find sustainable technologies which are economically competitive, as it pretends to be the studied reaction in the future.

Also, the obtention of fructose from biomass, which is composed from non-edible crops, ends with the competition for edible crops that generate other processes, with the rise prices in aliments that suppose. This could be included in “People”, that determines we must end with poverty and hunger. This process applied in industry would not end with hunger, but being applied instead of others can avoid the damage of the cycle of edible crops.

1. INTRODUCTION

1.1 - BIOFUELS IN OUR SOCIETY

Industry must change, our planet cannot sustain much more time this consumption and production rhythm, and therefore the search for renewable and sustainable alternatives is one of the biggest challenges of our society nowadays.

The fuel industry is one of the most widespread and pollutant, so reducing its environmental impact is key to making a noticeable improvement. In addition, there is an impending depletion of fossil fuel resources that has forced some climate chance policies, which have led to the development of more sustainable fuel sources, biofuels. Biofuels are defined as any fuel proceeding from any organic material part of the biomass.

Biofuels are divided into primary and secondary biofuels [1]. The primary ones have been used by humans since prehistoric times for cooking, lighting and heating. They are organic material mainly used in their unprocessed form, and include firewood, woodchips, wood pellets and wood charcoal. On the other hand, secondary biofuels are obtained processing biomass, usually used for vehicles or industry processes. In this case, they are divided into first, second and third generation depending on its raw material and which technology was used on their production.

First generation biofuels come from food or animal feed crops and are produced through well-known technologies as fermentation or distillation. However, they are leading to a controversial debate about the social impact that can make the redistribution and demand growth of agricultural land, which can suppose a price rise.

Second generation biofuels are those produced from non-edible crops like agricultural lignocellulosic biomass, so the agricultural land competition for food supplies of the first-generation ones is eradicated. Also, they wipe out some of the pollution that entails the demand growth [2]. However, there are not yet produced commercially because their technologies are not cost competitive compared to first generation biofuels or fossil fuels.

Third generation biofuels are those derived from microalgae, but their production is energy-intensive, what makes them economically unviable.

1.2 - FROM BIOMASS TO BIOFUELS

Fuels from sugars can be obtained directly by fermentation, leading mainly to bioethanol. Bioethanol has some drawbacks to be a substitute of gasoline, such as the low energy density and relative low boiling point of ethanol. Hence, the search of alternative chemical catalytic conversion processes [15].

The three main catalytic routes to transform biomass into fuels and chemicals are gasification, pyrolysis and hydrolysis, as can be seen in Figure 1.

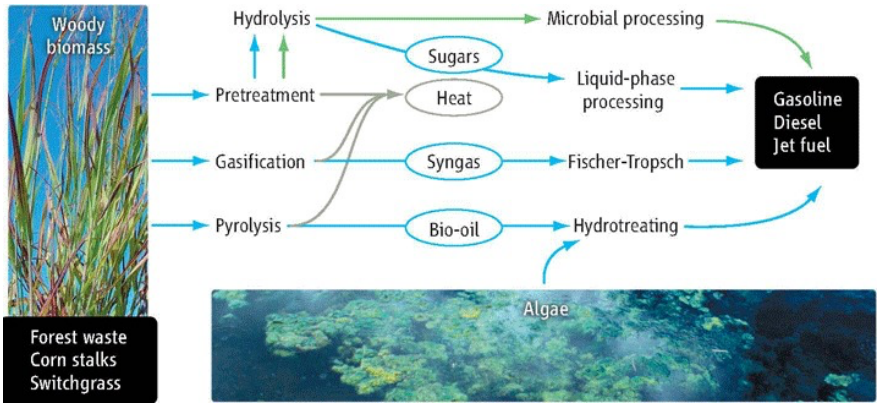

Figure 1. Routes to transform biomass into fuels [3].

Hydrolysis-based methods exclusively concede the production of a wide range of fuel components and chemicals and have the advantage of mild reaction conditions, what makes easier the control.

Hydrolysis consists of releasing biomass sugars from their lignocellulosic matrix. Lignocellulosic is an abundant and inexpensive feedstock, composed of lignin (15-20%), hemicellulose (25-35%), a polymer formed of C5 and C6 sugar monomers, and cellulose (40-50%), a polymer of glucose units. The goal is to liberate cellulose from lignin and hydrolyze it into glucose monomers. However, the main function of lignocellulosic is to avoid microbial and enzymatic degradation, which complicates this fractionation, so it requires some pre-treatments that represent more than 45% of the total cost of biofuel production.

These obtained sugars are converted into platform molecules, which are then converted into fuel additives through catalytic transformations such as esterification or etherification, among others.

1.3 - PLATFORM MOLECULES

Platform molecules are those derivable from biomass that can be utilized as building blocks for higher-value chemicals [5]. The most outstanding ones are furfural (2-furaldehyde), 5-hydroxymethyl-furfural (HMF) and Levulinic Acid (LA).

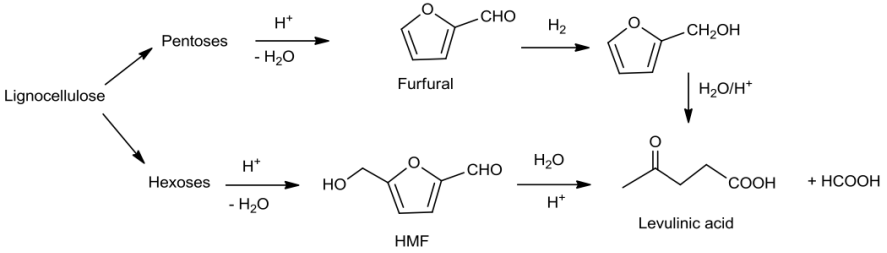

Figure 2. Biomass derived platform molecules from dehydration of monosaccharides [16].

As seen in figure 2, furfural is derived from pentoses and can be used as raw material for the obtaining of several non-petroleum derived chemicals as furfuryl alcohol and furan.

HMF derives from hexose carbohydrates, in a dehydration reaction with alcohols and solid acid catalysts. Is known for its dehydration properties, which have made it an essential nexus to obtain liquid biofuels, so that is considered the key intermediate between biomass and biofuels. Despite glucose is more inexpensive than fructose, using fructose to obtain HMF is more favorable in terms of conversion and selectivity. Hence, the studied reaction starts from fructose.

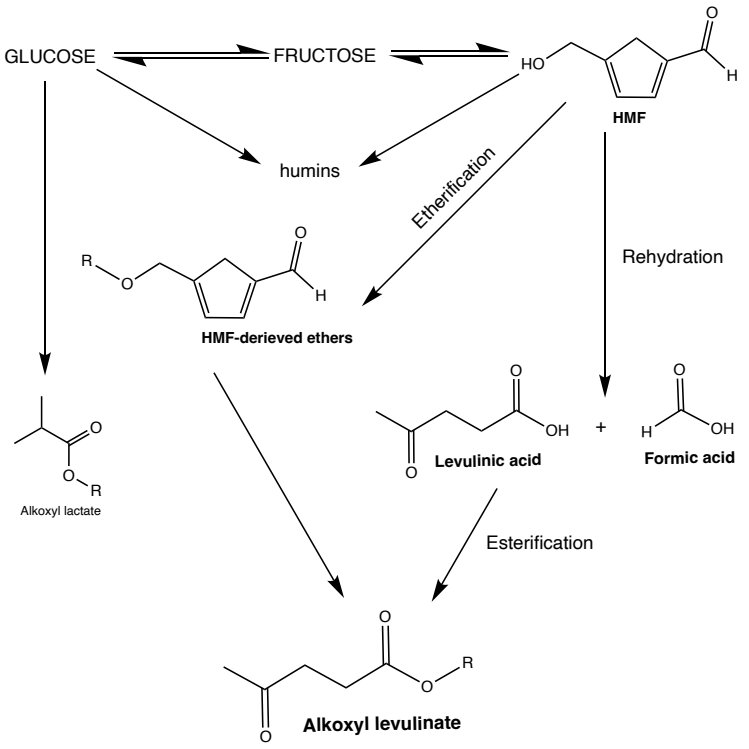

Firgure 3. Molecular transformations from fructose to alkyl levulinates.

The main drawback of this process are side reactions that lead to undesired products such as insoluble humins, affecting the catalyst to such an extent that their formation determines the yield of the reaction. As seen in figure 3, humins come from fructose degradation and HMF catalytic reactions and they can cause blockage of pipes and other equipment.

HMF can be converted in many oxygenated compounds used as biofuels or biofuels additives, as shown below in Figure 4. Even so, many platform molecules are highly oxygenated compounds, and they require partial oxygen removal in their conversion to biofuels.

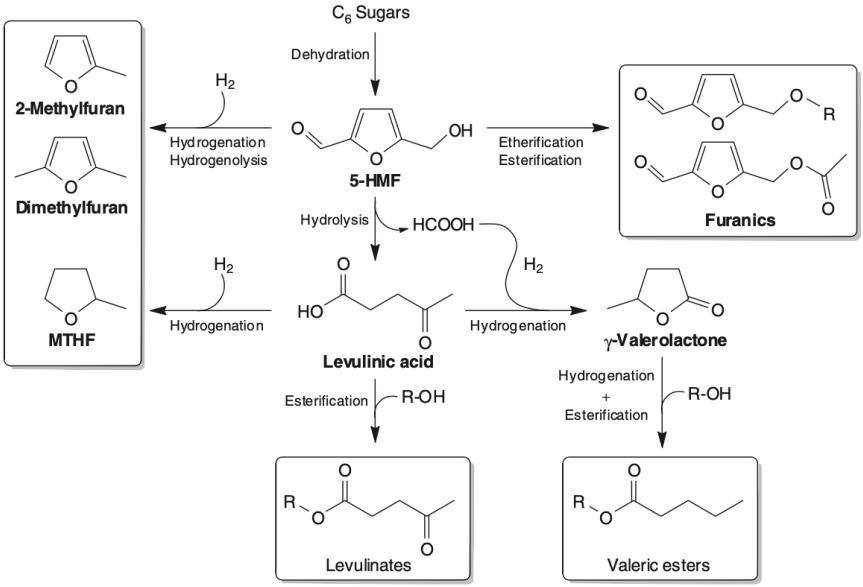

Figure 4. Routes to produce oxygenated compounds from HMF [15].

Levulinic acid (LA, 4-oxopentanoic acid) is considered one of the most important platform molecules derived from biomass, and it outstands for its reactive nature. Their interesting properties are known since 1870, but its commercial use didn't detach until its obtaining process (raw material price, yield, purification, etc.) was economically profitable.

Nowadays, the acquiring of LA from lignocellulose biomass is highly attractive due to its abundance and low cost, and because it doesn't disturb food production. It is obtained from the hydration of HMF with two molecules of water, following the scheme bellow (Figure 5).

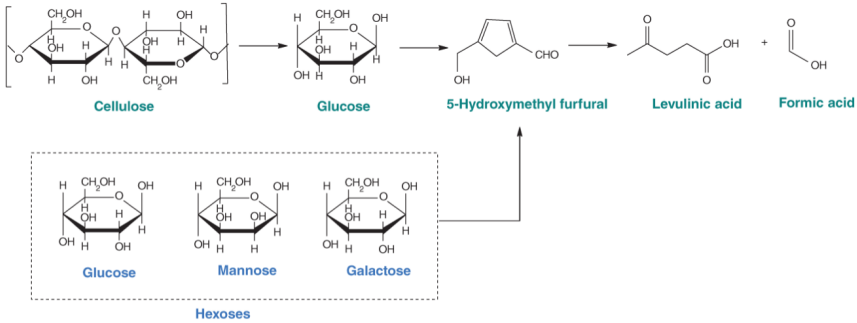

Figure 5. Route for the formation of LA from simple sugars. [6]

LA production has relatively high yields (higher than 60%), but its production is accompanied by an equal amount of formic acid.

Is identified as a promising material for the synthesis of great industrial application, such as coating resins, in food applications as pH regulator, polymers, corrosion inhibitors, electronics, etc. LA derivates are also promising, especially esters of levulinic acid for their possible application as biofuel additives, which brings them to a lower range of pricing.

Industrially, the Biofine process (Fitzpatrick, 1990,1997) is one of the most advanced and commercially viable lignocellulose-fractionating technology, in part because it does not produce glycerol as a co-product [15]. Nowadays LA is still expensive to produce, but the price is expected to fall as the conversion technologies are commercialized, and then its use is expected to increase.

1.4 - ALKYL LEVULINATES

Alkyl levulinates (ALs) are of particular interest for their specific physicochemical properties and low toxicity, which have the potential to substitute current chemicals produced from petrochemical routes as additives to current diesel or gasoline. They have a large spectrum of applications, as solvents since they are soluble in classical solvents (alcohols, ethers and chloroform) and as additives to polymers, perfumes, flavoring preparations or latex coating compositions [11]. In fact, their use has been patented for mineral oil refining. Although, the main potential and attractive application is as fuel additives.

There are different routes to obtain ALs (seen in Figure 6). The most known way is the esterification of levulinic acid with alcohols, due to its high yield and selectivity, but the reaction must be acid catalyzed because of its slowness [7]. Alkyl levulinates can also be obtained by the reaction of furfuryl alcohol (derived from furfurals reduction) with an alcohol in presence of acid or directly from lignocellulosic resources with more limited yields [8].

However, the alcoholysis of simple sugars, such as fructose, is the way with more advantages since it requires less post-treatment operations [4].

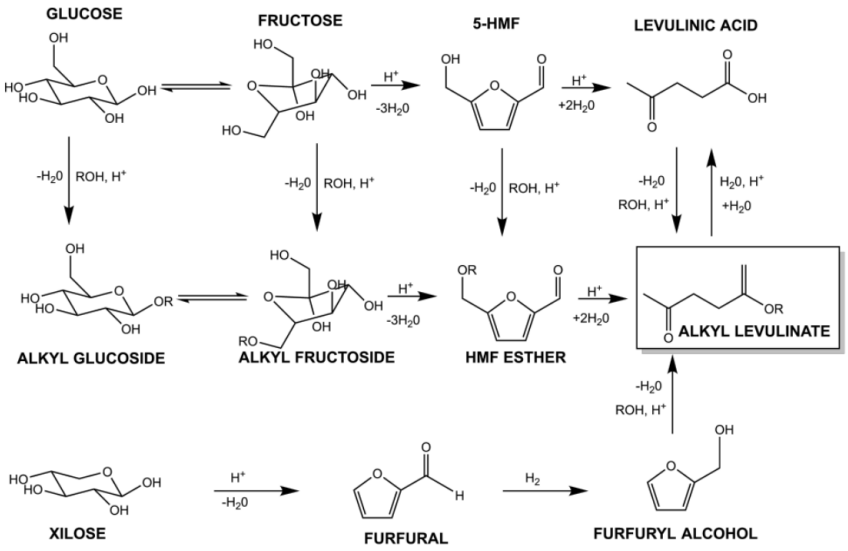

Firgure 6. Different synthesis pathways to obtain alkyl levulinates [10].

To be considered good biofuels, they must meet a minimum of requirements, such as have its melting point a way lower than ambience temperature or provide an adequate burn rate, neither too fast or to slow, to avoid both overheating and not boiling over.

Cetane number (CN) is a measure of the ignition delay of a diesel fuel [10]. The higher the CN, the shorter the interval between the time the fuel is injected and the time it begins to burn.

Ethyl levulinate is the most studied AL, followed by butyl levulinate. The main advantage of their use instead of conventional additives is that they lead to cleaner combustion and enhance fuel quality. That is due to their oxygenated nature and their capacity as cold-flow improvers in biodiesel. On the other hand, the principal disadvantage is its poor low temperature operability [9]

Butyl levulinate is the most promising diesel blend component [4]. It has a higher cetane number, and it is much less soluble in water, and more miscible with diesel than ethyl levulinate. Also, it improves cold flow properties, conductivity, lubricity and reduce its vapor pressure. Beyond biofuels, butyl levulinate has also applications as bio-based auxiliary plasticizer [20] and as a solvent.

1.5 - ACIDIC ION-EXCHANGE RESINS AS HETEROGENOUS CATALYST

The drawbacks of homogenous catalysts have led them to be replaced despite the advantages they offer, such as their accessibility to active sides, activity and selectivity. Their corrosion problems, difficulty to separate them from the rest of the products and lack of reusability have reduced its industrial application to a 20%. Instead, the use of heterogenous catalyst occupies the other 80% of which a 90% are solid catalysts [13]. Heterogenous catalysts allow working under higher temperatures, what makes shorter time reactions and avoids the degradation of HMF. Also, they outstand for the ease of separating them from the product and the possibility of being recycled. [15]

Solid catalyzed reactions elementary steps are Adsorption, surface Reaction and Desorption. The reaction occurs in specific places of the catalyst surface called active sites. Adsorption can be the rate-limiting step since surface area is one of the most remarkable limitations of this kind

of catalyst. Thus, in purpose of catalysts with an extended surface, most of them are porous solids.

Usually, solid catalysts have been valued in terms of activity, selectivity, lifespan and reusability. To obtain biofuels from biomass have been used different type of solid catalysts, micro-mesoporous materials, metal oxides, supported metal catalysts and sulfonated polymers. Among them, acidic ion-exchange resins have been of particular interest [14].

Acidic ion-exchange resins have a cross-linked matrix compost of copolymers of styrene, divinylbenzene (DVB) and sulfonic acid groups grafted on benzene rings of styrene. As any functional resins, they are produced in two morphological types [12]:

1. Microporous (Gel-type): resins without porosity in the dry state (thus, a reduced surface area) and low-crosslinked. The pores only appear on polar solvents after a high degree of swelling.
2. Macroporous (Macroreticular): resins with stable porosity in dry state and high-crosslinked.

The matrix is where the functional groups can be found, and it is cross-linked with DVB to give the polymer a tridimensional structure. The cross-linking degree is given by the proportion of reticulating agent (DVD) (wt.%), which is related with the thermal and mechanical resistance and porosity. High cross-linked polymers are associated with more stiff, strong and more brittle structures, but they can present internal mass transference problems. While the low cross-linked ones with softer, more elastic and mechanically unstable structures.

The knowledge of swollen-state morphology is key to understand resins behavior, due to its huge impact to their catalyst properties. The behavior of each resin can be seen in figure 7:

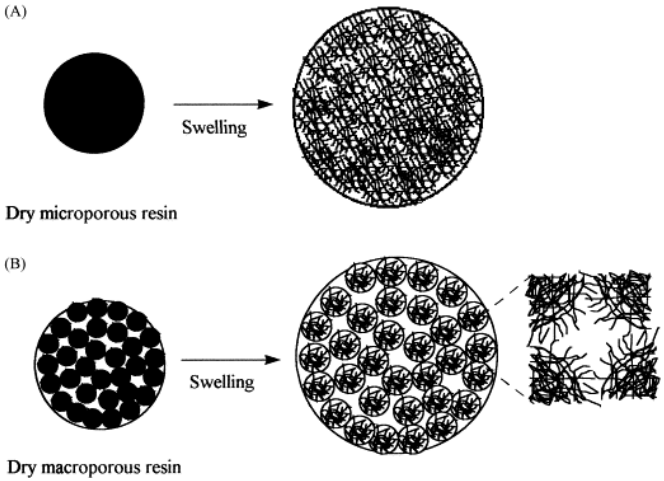

Figure 7. Representation of chances in the morphology of microporous (A) and macroporous (B) polymers during swelling [12].

As mentioned, humins formation comes hand in hand with the fructose degradation. Which can explain the loss of activity on a resin weight basis because of the desulfonation and fouling [11].

Ramírez et al. [11], [14] concluded that lower content of cross-linked agent leads to higher yields, both for fructose dehydration to levulinic acid and for direct esterification of levulinic acid with alcohols. Hence, Dowex 50Wx2, 2% DVB is the resin used in the studied reaction. Although, for reasons beyond our knowledge this study is lack of a kinetic model, which is essential for a future industrial application.

2. OBJECTIVES

As mentioned in introduction, a kinetic study is crucial for the implementation of a process to industrial scale, which lacks nowadays in the literature for the obtention of BL from fructose.

This study is a contribution to larger research that has been studying, for years, different aspects of this reaction network (i.e. the optimum resin used) focused on kinetics.

The goal is to search for a kinetic preliminary model that describes the reaction behavior as a preliminary step for a future deeper kinetic study. For this purpose, the aim of this work is to find:

- Reaction rates of formation for every compound
- Kinetic constants of reactions involved at each temperature.
- Activation energy for each reaction.

With this purpose, the data used for this work has been taken from *A contribution to the study of acidic ion-exchange resins to produce butyl levulinate from fructose and butyl alcohol* [18].

3. STUDIED REACTION AND CONDITIONS

3.1 - STUDIED REACTION NETWORK

The studied reaction network is the following:

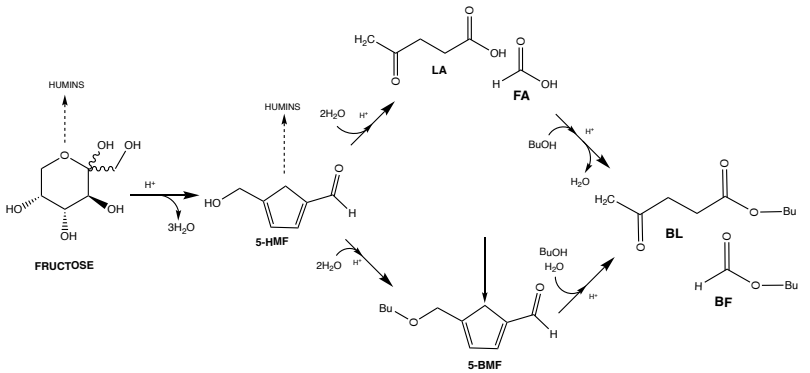

Figure 8. Catalytic reactions for the synthesis of butyl levulinate from fructose.

First, fructose is dehydrated to HMF. For this purpose, it is needed a stable solvent capable of dissolving the sugar, along with a heterogeneous catalyst, already mentioned, and a suitable temperature range. If possible, it is preferable working under mild conditions, however, selection increases as it does temperature, probably because side reactions have lower activation barrier [17]. In this case, experiments have been made between 80 to 120 ºC and the used solvent has been 1-butanol.

It has been chosen 1-butanol because in addition to dissolve fructose properly, it acts as a second reagent in the esterification of levulinic and formic acids (see Figure 8). This implies the need to introduce fewer compounds in the reactor.

The amount of sugar in the influent can be also determinant since too high concentrations can lead to side reactions, causing selectivity to drop.

Then is produced the HMF hydration to levulinic and formic acids, and the etherification to 5-butoxymethylfurfural (BMF) in parallel. One mole of fructose can produce one mole of LA, and the hydration must be, at least, with two molecules of water for every molecule of HMF [6]. However, high concentrations of 1-butanol favour the formation of BMF.

Finally occurs the LA and FA esterification to butyl levulinate (BL) and butyl formate (BF), that consists in the protonation of the carbonyl oxygen atom of LA or FA, which allows a further nucleophilic attack of the alcohol, and this leads to a quaternary carbon atom [16].

Levulinic acid esterification is a reversible reaction, which means that a high LA conversion is achieved practically in the equilibrium conversion. This high conversion is obtained with stoichiometric excess of 1-butanol (ranging from 3 to 10) and ideally removing the formed water to shift the equilibrium and avoid its inhibitory effect on the catalytic activity of the resin [19], but in these experiments remains it in the reactor.

3.2 - STUDIED REACTION CONDITIONS

As mentioned, it is meant to study the kinetic behaviour of the reaction and determine its kinetic constants. Nevertheless, it should be noted that kinetic constants depend on the temperature, so this study only describes the reaction conduct on these specific conditions, which are explained below.

As reagent was used fructose (99%, labkem) accompanied by 1-butanol (99.5%, Acros Organics) and water (Milli-Q, Millipore) with no prior purification. For chromatographic calibrations, the reagents used were also 1-butanol, levulinic acid (98%, Acros Organics), formic acid (98%, labkem), butyl formate (98%, Acros Organics), butyl levulinate (98%, ALDRICH), 5-hydroxymethyl-furfural (98%, Acros Organics), di-butyl ether (99%, Acros Organics).

It was used a stirred tank reactor pressurized by nitrogen gas (99,99% of purity, Abelló Linde) up to 21 atm. Reaction samples were analysed by gas chromatography and high liquid performance chromatograph (HPLC) simultaneously, and the carrier gas used at gas chromatograph was helium (99,99% of purity, Abelló Linde).

The acidic resin used was Dowex 50Wx2, a gel-type resin with a cross-linking degree (% DVB) of 2%, and it was conventionally sulfonated. Important properties of this resin are specified in Table 1.

Dowex 50wx2

Type	Gel
Sulfonation type	Conventionally Sulfonated
Acid capacity (mmol H+/g)	4.83
% DVB	2
d_p^c (mm)	0.149
Water retention (%)	74-82
T_{max} (ºC)	150
d_{pore} (nm)	-
ΣV_{pore} (cm^3/g)	-
Σs_{pore} (m^2/g)	-
ΣV_{sp}^e (cm^3/g)	2.677

Table 1. Properties of Dowex 50Wx2.

All experiments were 8h long with the temperature constant through the reaction and in liquid phase. Also, all of them started with the same composition of the initial load, which is: 2.5 (wt %) Fructose, 16 (wt %) Water and 81.5 (wt %) 1-Butanol.

The setup and procedure are carefully described in *A contribution to the study of acidic ion-exchange resins to produce butyl levulinate from fructose and butyl alcohol* [18] the study from which the data for this work has been taken.

The obtained data are shown in figure 9, which is the basis of this work:

A

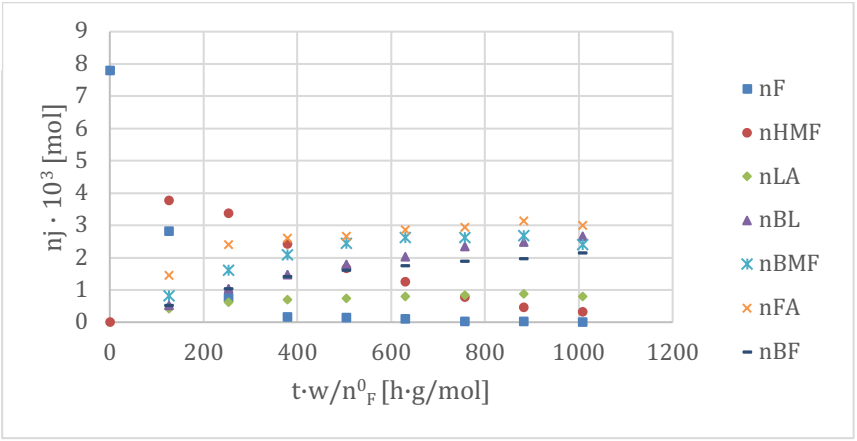
nj · 10³ [mol]
t·w/n⁰F [h·g/mol]
nF
nHMF
nLA
nBL
nBMF
nFA
nBF

B

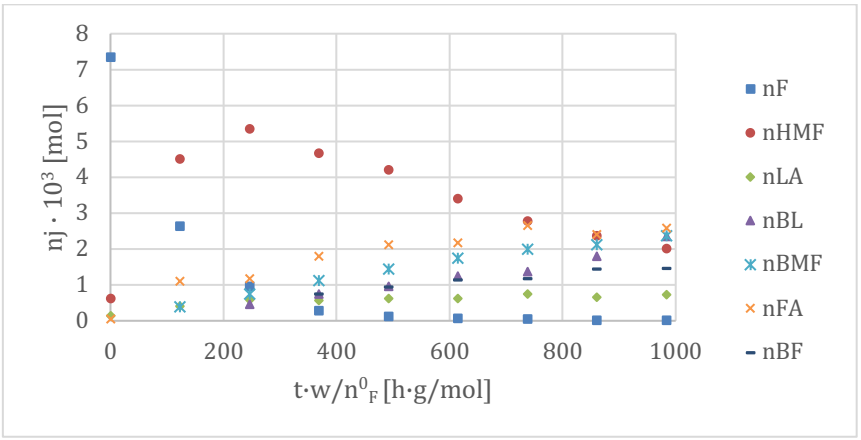
nj · 10³ [mol]
t·w/n⁰F [h·g/mol]
nF
nHMF
nLA
nBL
nBMF
nFA
nBF

C

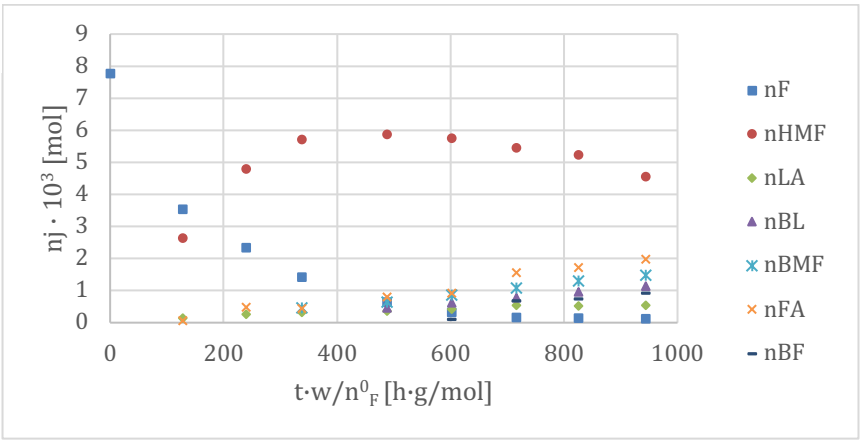
nj · 10³ [mol]
t·w/n⁰F [h·g/mol]
nF
nHMF
nLA
nBL
nBMF
nFA
nBF

D

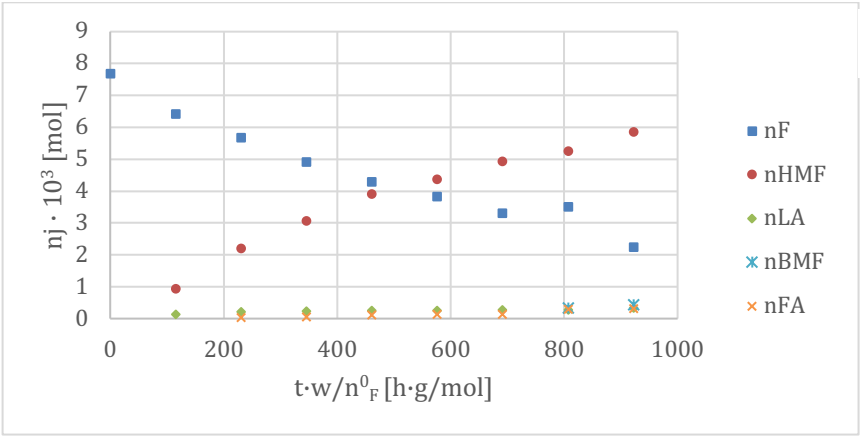
nj · 10³ [mol]
t·w/n⁰F [h·g/mol]
nF
nHMF
nLA
nBMF
nFA

E

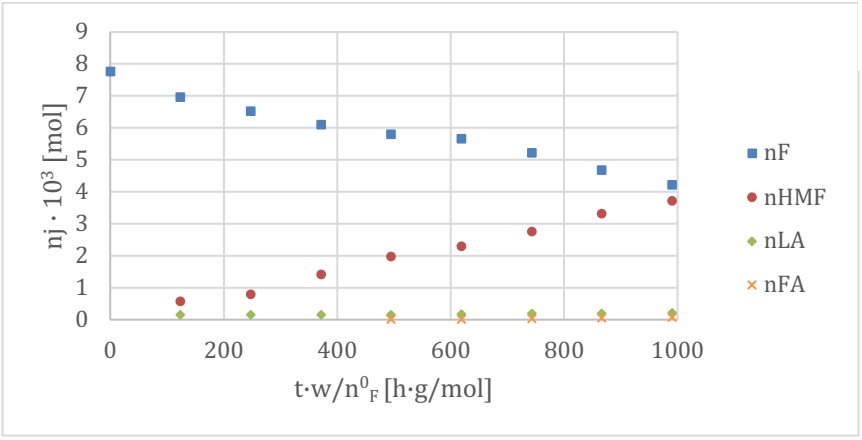
nj · 10³ [mol]
t·w/n⁰F [h·g/mol]
nF
nHMF
nLA
nFA

F

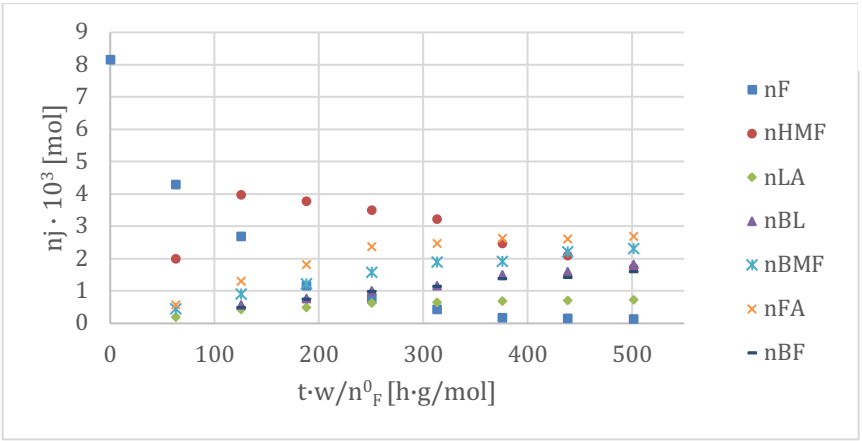
nj · 10³ [mol]
t·w/n⁰F [h·g/mol]
nF
nHMF
nLA
nBL
nBMF
nFA
nBF

G

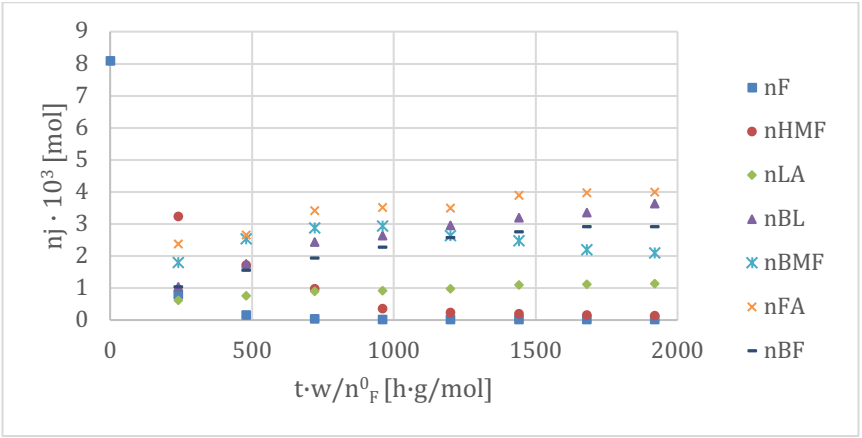

H

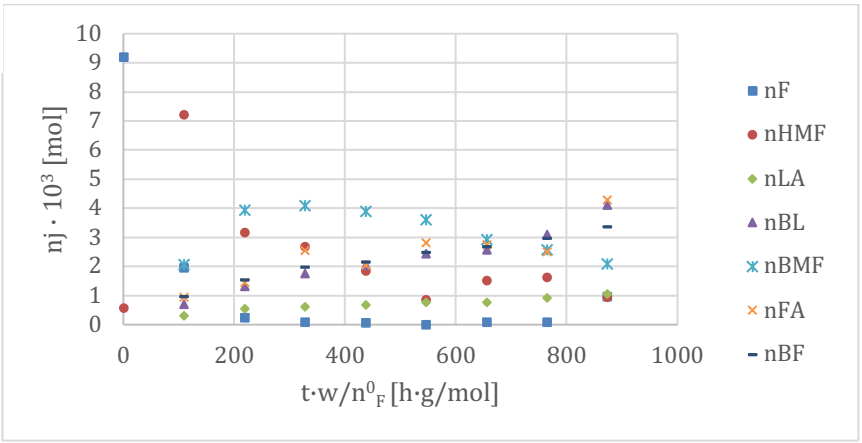

Figure 9. Experimental mole variation throughout time.
A: 120ºC, 1g catalyst and 0.0078 mol_{F^o},
B: 110ºC,1g catalyst and 0.0073 mol_{F^o},
C: 100ºC, 1g catalyst and 0.0078 mol_{F^o},
D: 90ºC, 1g catalyst and 0.0077 mol_{F^o},
E: 80ºC, 1g catalyst and 0.0078 mol_{F^o},
F: 120ºC, 0.5g catalyst and 0.0081 mol_{F^o},
G: 120ºC, 2g catalyst and 0.0081 mol_{F^o},
H: 120ºC, 1g catalyst and 0.0092 mol_{F^o}.

Mole concentration of 1-butanol (BuOH) and water have been considered constants. This is due to their high values compared to the other compounds. Table 2 shows their concentration of each experiment.

Experiment	BuOH [mol/L]	H_2O [mol/L]
1 (A)	8.44 ± 0.03	7.1 ± 0.2
2 (B)	8.58 ± 0.06	7.1 ± 0.2
3 (C)	8.72 ± 0.07	6.9 ± 0,1
4 (D)	8.52 ± 0.03	7.08 ± 0.06
5 (E)	8.74 ± 0.03	7.4 ± 0.1
6 (F)	8.54 ± 0.01	6.9 ± 0.1
7 (G)	8.38 ± 0.04	6.89 ± 0.09
8 (H)	9.27 ± 0.05	4.6 ± 0.3

Table 2. Average concentration of BuOH and H_2O for all experiments.

4. RESULTS AND DISCUSSION

It is important to mention that this work is based on the search of an ideal pseudo-homogeneous model, what means that the material transportation effects are not considered. This is because is the further that can be gone with the data on hand, and because it is a good approximation for a preliminary model as this one is. In consequence, concentrations are used instead of activities throughout the calculation.

Applied kinetics is based on obtaining a rate reaction expression that describes the changes of composition over time. The reaction rate of formation of a compound j (r_j) is described as the variation of concentration through time. Since reaction rates are not known in the available data, it is necessary to estimate them first.

4.1 - ESTIMATION OF THE REACTION RATES

For a compound j in a heterogeneously catalyzed reaction, the reaction rate of formation or decomposition can be defined as:

$$r_j = \frac{1}{w} \cdot \frac{dn_j}{dt} \left[\frac{mol}{h \cdot g}\right] \quad (1)$$

Note the importance that has the amount of catalyst in the reaction, and how its determinant for the reaction rate. Although, in the available data this amount is already settled, so the study goes around the variation of moles through time.

To carefully display the methodology followed in the reaction rates of formation obtentions, one of the experiments will be explained in detail step by step as an example. It is taken as an example fructose (F) evolution in the 1st experiment:

To model the variation of fructose moles with time, empirical models have been fitted to describe the variation of moles over time. To find a mathematical model that describes the behaviour of the curve, the chosen model must meet two requirements:

- It must fit the data as faithfully as possible. To achieve this, it has been used the least squares method, which consists in calculating the square of the error (the difference between the known value and the calculated value). As the lower is the least squares value, the better is fitted the data.
- The later calculated reaction rate must make physical sense. That implies to be consistent depending on the paper of the compound in the reaction, if it is a reagent, a product or an intermediate product. For example, it has no sense for a product, which is the main goal of the reaction, to have a negative reaction rate of formation, because that would mean its decomposition instead of its formation.

With these two requirements in mind, the model is chosen. There is not a set value of least squares to determine from where is considered acceptable, and this is due to each component of each experiment has its own fit and not all of them have the same accuracy.

It is to be noted that independent term is contact time and not time. This contact time (t_c) is described as:

$$t_c = \frac{w \cdot t}{{n_F}^o} \left[\frac{g \cdot h}{mol}\right] \qquad (2)$$

As seen in equation (2), contact time considerate the amount of catalyst used and the initial concentration of fructose, the main reagent.

As a result, reaction rates are not described as usual, they are described as:

$$r_j = \frac{1}{W}\frac{dn_j}{dt} = \frac{1}{n_F^o}\frac{dn_j}{dt_c}\left[\frac{mol_j}{g \cdot h}\right] \quad (3)$$

All the empirical models used for the different compounds at different temperatures, can be seen in Appendix 2, with the used parameters and their confidence interval. Also, the equation of each model is seen in Appendix 1.

For the fructose evolution in the 1st experiment, it has been seen that those models that fitted better the curve, and in consequence, had a lower value of least squares were the following.

Model	Equation	Parameters	Least squares
Ratkowsky	$n = \frac{a}{1 + e^{b - c \cdot t_c}}$	a = 0.02	**1,64487E-08**
		b = 0.2	
		c =-0.011	
MMF	$n = \frac{ab + ct_c{}^d}{b + t_c{}^d}$	a = 0.008	**7,30706E-08**
		b = 90802	
		c = -2.4E-05	
		d = 2.5	
Exponential decline	$n = q_0 e^{\frac{-t_c}{a}}$	a = 0.008	**7,30706E-08**
		q_0 = 116.9	

Table 3. Different fit models for the Fructose in the 1st experiment. Dowex 50Wx2, 120ºC, 1 g catalyst.

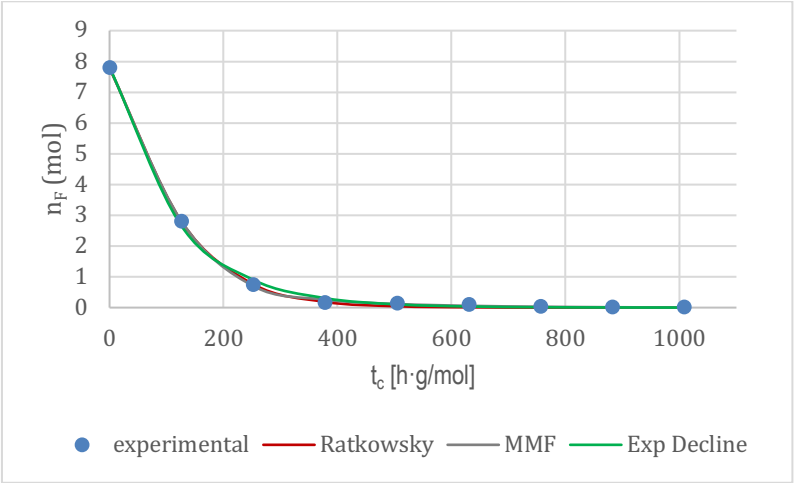

Figure 10 Different fit models that describe the moles variation of fructose in 1st experiment. Dowex 50Wx2, 120ºC, 1 g catalyst.

As seen in table 3, the least squares of the three models are of the same order of magnitude and they fit quite well. Although, this is not enough criteria to choose any of them.

As said, another essential requirement to determine a model to describe the behavior of a component through time, is that its reaction rate makes physical sense. Fructose is the main reagent of the reaction, so its reaction rate must be higher at the beginning and decrease as it does the fructose concentration.

According to equation (1) to estimate the reaction rate of formation of a compound, the derivative of the model that describes the data is made. Using this equation, the following fructose reaction rates have been obtained for the three different models:

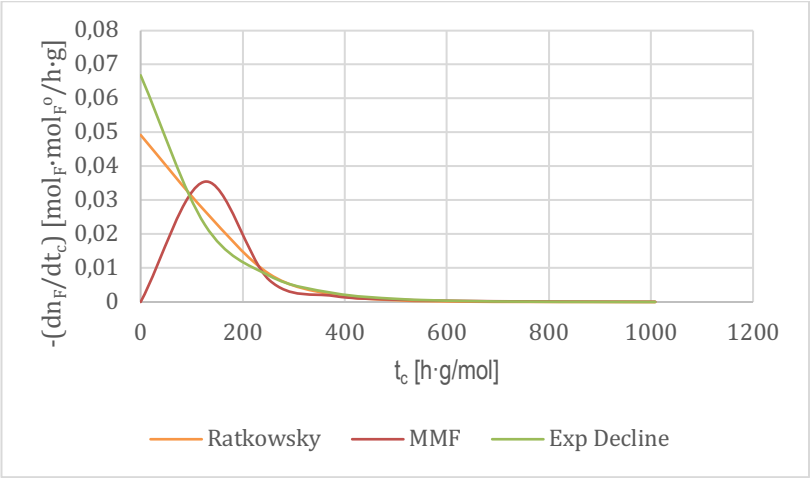

Figure 11. Fructose reaction rate for different fit models in 1st experiment. Dowex 50Wx2, 120ºC, 1 g catalyst.

Figure 11 shows that the MMF model does not describe the fructose rate as expected. The initial maximum that presents makes mathematical sense but not physical sense. Fructose initial rate cannot be zero or the reaction would not take place, so MMF is excluded as a possible fit model for fructose in this experiment.

The two remaining models can be a good fit for the behavior of fructose in this experiment as they meet both requirements. As said, the criteria to choose a model is the one with least squares value, so Ratkowsky model is the selected model for fructose since it has the lower value.

Following this procedure in all cases, figure 12 (A to H) shows the variation of reaction rate of formation of each species j against tc. According to equation (3), y-axis of each figure represents the product $n_{F^o} \cdot r_j$.

.

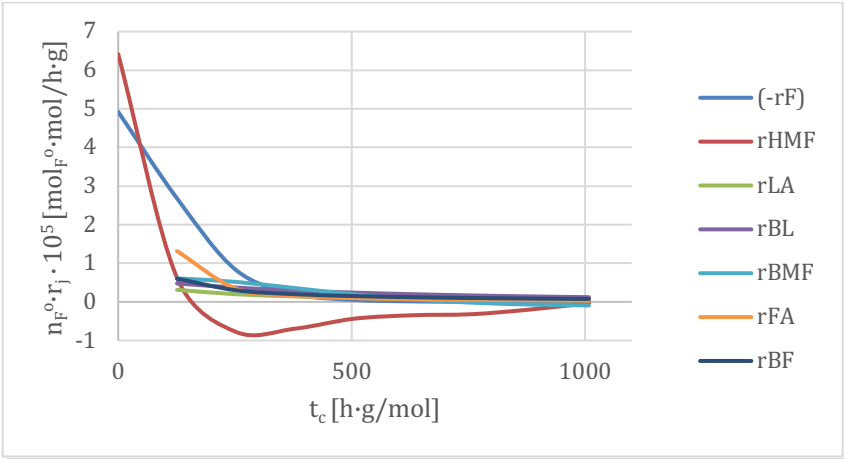
A
$n_F^o \cdot r_j \cdot 10^5$ [$mol_F^o \cdot mol/h \cdot g$]
7
6
5
4
3
2
1
0
-1
0
500
1000
t_c [h·g/mol]
(-rF)
rHMF
rLA
rBL
rBMF
rFA
rBF

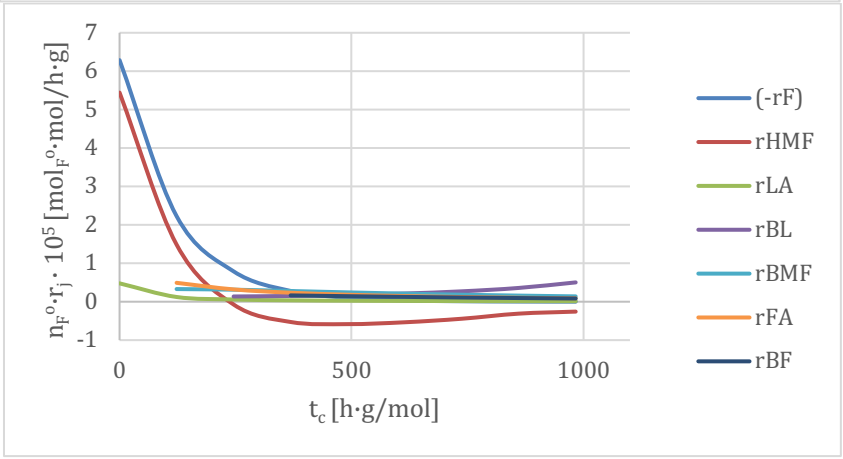
B
$n_F^o \cdot r_j \cdot 10^5$ [$mol_F^o \cdot mol/h \cdot g$]
7
6
5
4
3
2
1
0
-1
0
500
1000
t_c [h·g/mol]
(-rF)
rHMF
rLA
rBL
rBMF
rFA
rBF

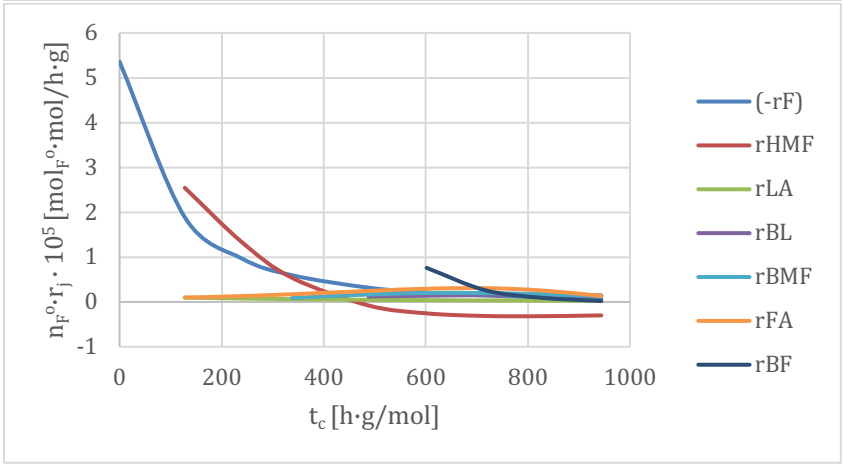
C
$n_F^o \cdot r_j \cdot 10^5$ [$mol_F^o \cdot mol/h \cdot g$]
6
5
4
3
2
1
0
-1
0
200
400
600
800
1000
t_c [h·g/mol]
(-rF)
rHMF
rLA
rBL
rBMF
rFA
rBF

D

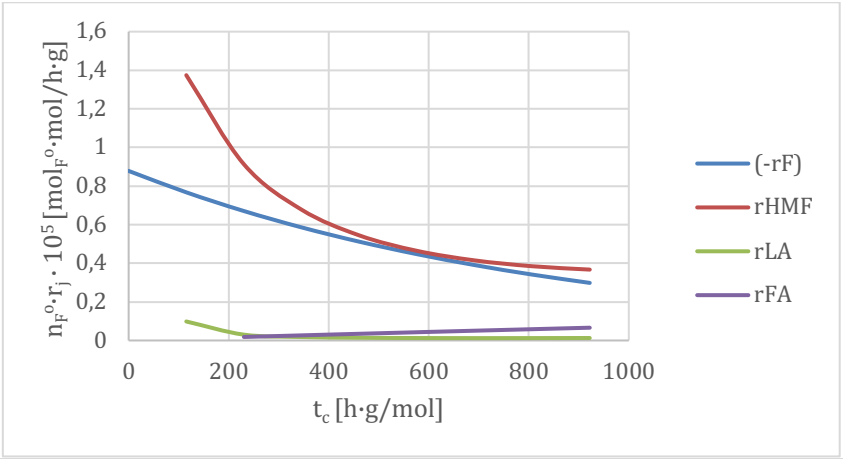
1,6
1,4
1,2
1
0,8
0,6
0,4
0,2
0
0
200
400
600
800
1000
$n_F^o \cdot r_j \cdot 10^5 [mol_F^o \cdot mol/h \cdot g]$
t_c [h·g/mol]
(-rF)
rHMF
rLA
rFA

E

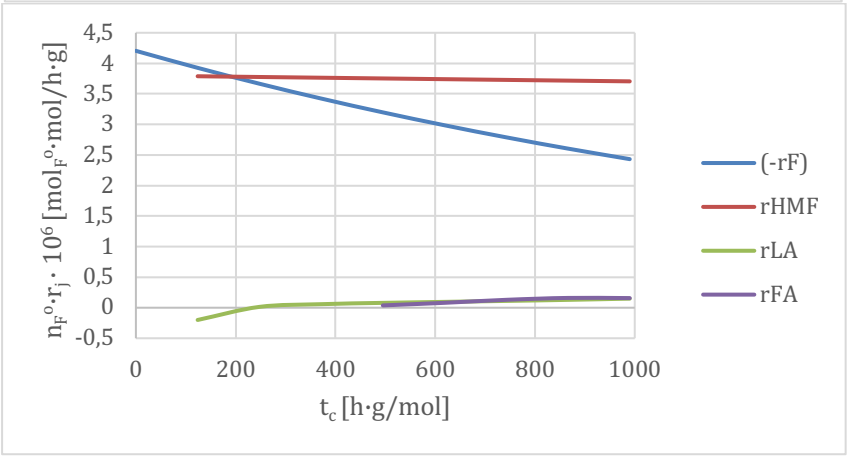
4,5
4
3,5
3
2,5
2
1,5
1
0,5
0
-0,5
0
200
400
600
800
1000
$n_F^o \cdot r_j \cdot 10^6 [mol_F^o \cdot mol/h \cdot g]$
t_c [h·g/mol]
(-rF)
rHMF
rLA
rFA

F

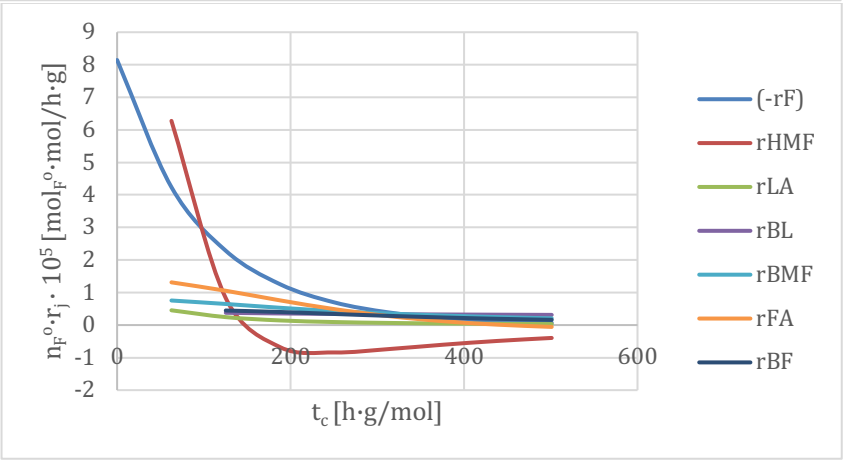
9
8
7
6
5
4
3
2
1
0
-1
-2
0
200
400
600
$n_F^o \cdot r_j \cdot 10^5 [mol_F^o \cdot mol/h \cdot g]$
t_c [h·g/mol]
(-rF)
rHMF
rLA
rBL
rBMF
rFA
rBF

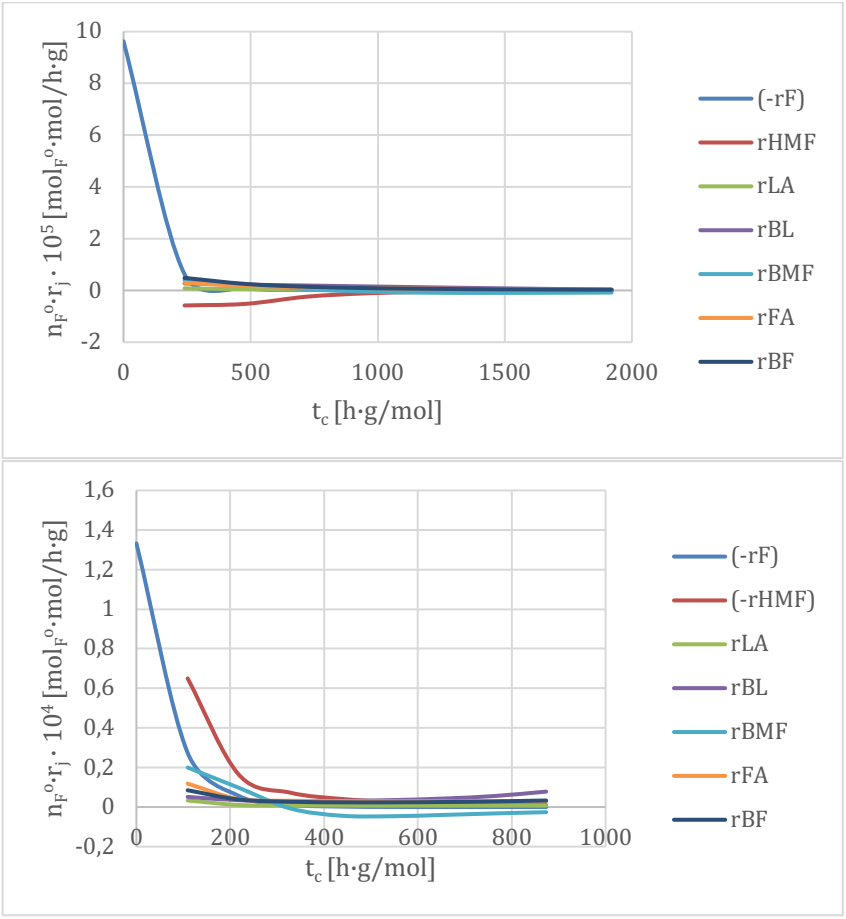

Figure 12. Calculated reaction rates by fit models.
A: 120ºC, 1g catalyst and 0.0078 mol_F^o,
B: 110ºC,1g catalyst and 0.0073 mol_F^o,
C: 100ºC, 1g catalyst and 0.0078 mol_F^o,
D: 90ºC, 1g catalyst and 0.0077 mol_F^o,
E: 80ºC, 1g catalyst and 0.0078 mol_F^o,
F: 120ºC, 0.5g catalyst and 0.0081 mol_F^o,
G: 120ºC, 2g catalyst and 0.0081 mol_F^o,
H: 120ºC, 1g catalyst and 0.0092 mol_F^o.

Note that for all compounds is represented its rate of formation except for fructose that is represented its opposite (the rate of decomposition). That is because fructose is the main reagent of the reaction and its rate of formation is always negative, which means that its moles are always decreasing.

Another compound that outstands is the HMF, which is an intermediate of the reaction. At the beginning, its rate as well as its composition should be zero, but this is not fulfilled in all cases. That might be because the dehydration of fructose to HMF started before the first sample was taken, were the time was considered zero. At the beginning, the reaction rate of formation should increase until it is formed, then HMF reaction rate should decrease which means that starts its rehydration. At the end the reaction rate is negative, which implies all formation is done and it is just left the dehydration.

The curve that presents is so different from one experiment to another because its mole variation is not completely defined in most of experiments, as seen in Figure 9. This is because the mole variation between samples is too high to define it properly. This can be seen in Appendix 2, where the confidence interval of HMF is one of the highest. For optimum results, it would be necessary to decrease the time between samples, and then the mole evolution of HMF would be better defined and their rates of formation as well.

In case H (8th experiment), it is also represented the rate of decomposition of HMF, that is because in the second sample it was already formed most of the HMF and was acting as the reagent for FA, LA and BMF.

Despite LA, FA and BMF are also intermediates of the reaction, their behavior is not as if they were in this figure. That is because their formation is much more scarce comparing with HMF. With the available data, in most cases is not appreciated the curve of previous formation and following destruction of these components for their transformation to BL and BF, but the procedure is the same as with HMF.

Just in 1st experiment, the FA curve is remarkable. But as it has happened with the HMF, its formation is not described in the data, because the sample was taken when it was already formed most of the FA.

Finally, BF and BL reaction rate is always positive, favoring their formation. This is because they are final products of the reaction. As seen in Figure 12, they are practically constant through time, this is due to such low values of their concentrations. In 3rd experiment (case C), is appreciable a maximum of the BF reaction rate, that is probably due to the experimental inaccuracy of the chromatograph for such diluted conditions.

Cases D and E have no values for some compounds because they were not detected in the chromatograph. Note that in both cases the fructose reaction rate decreases slower than in the other experiments, and in consequence, the rehydration of HMF is also slower. The lack of HMF causes than the reaction cannot continue and final products, or even other intermediates are not formed. In case E this event is even more pronounced. That is because of the temperature. Both experiments were made at temperatures lower than 100ºC. As mentioned, low temperatures favor side reactions as humins formation, which could explain this behavior.

4.2 - DETERMINATION OF KINETICS CONSTANTS

Kinetic constants (k) relate the reaction rate (r) with the composition, and they exclusively depend on the temperature

The studied reaction network is described by the following scheme reaction:

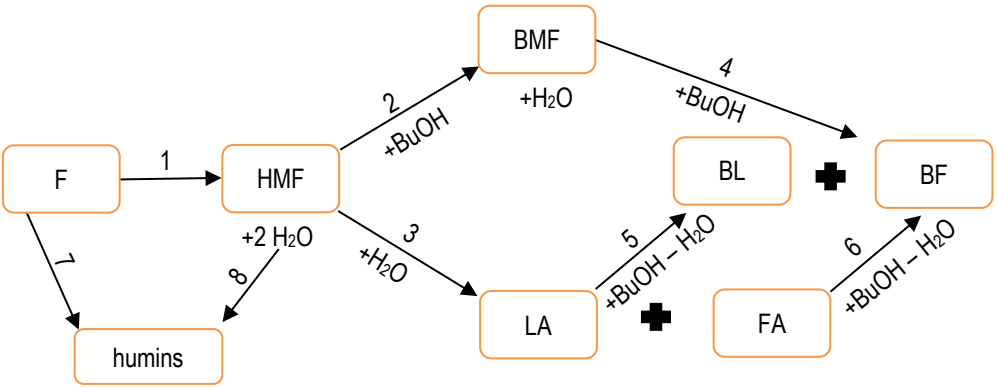

Figure 13. Scheme of the studied reaction.

Following the reaction scheme (Figure 13), and considering the model as pseudo-homogenous, rates of formation can be described as:

$$r_F = -r_1 - r_7 = -k_1 \cdot c_F - k_7 \cdot c_F \quad (4)$$

$$r_{HMF} = r_1 - r_2 - r_3 - r_8 = k_1 \cdot c_F - k_2 \cdot c_{HMF} \cdot c_{BuOH} - k_3 \cdot c_{HMF} \cdot c_{H_2O} - k_8 \cdot c_{HMF} \quad (5)$$

$$r_{BMF} = r_2 - r_4 = k_2 \cdot c_{HMF} \cdot c_{BuOH} - k_4 \cdot c_{BMF} \cdot c_{BuOH} \quad (6)$$

$$r_{LA} = r_3 - r_5 = k_3 \cdot c_{HMF} \cdot c_{H_2O} - k_5 \cdot c_{LA} \cdot c_{BuOH} \quad (7)$$

$$r_{FA} = r_3 - r_6 = k_3 \cdot c_{HMF} \cdot c_{H_2O} - k_6 \cdot c_{FA} \cdot c_{BuOH} \quad (8)$$

$$r_{BL} = r_4 + r_5 = k_4 \cdot c_{BMF} \cdot c_{BuOH} + k_5 \cdot c_{LA} \cdot c_{BuOH} \quad (9)$$

$$r_{BF} = r_4 + r_6 = k_4 \cdot c_{BMF} \cdot c_{BuOH} + k_6 \cdot c_{LA} \cdot c_{BuOH} \quad (10)$$

* All partial reaction orders have been considered 1, since it is found as the optimum value.

Bearing in mind that concentrations of different compounds through time are known (seen in Appendix 3) and reaction rates have been estimated in the previous section, kinetic constants can be calculated.

Note that the reaction rate of formation or decomposition for a compound j can be easily calculated knowing (dn_j/dt_c), according to equation (3).

To carefully explain the procedure and following the previous example, fructose rate of the 1st experiment is explained.

Once again is used least squares method to determine the kinetic constants value. The goal is to find the kinetic constants implied on the studied compound reaction, in this case fructose. According to equation (4), k_1 and k_7 are the ones involved in fructose formation, so the aim is to find those constants that present the lower least squares value between the calculated reaction rates with the mentioned equation and the estimated in the previous section, such as:

$$\Sigma\left(r_{j\ estimated} - r_{j\ calculated}\right)^2 \qquad (11)$$

To find the kinetic constants that minimize this summation, it is necessary an iterative calculation. This iterative calculation has been made starting from different values, to ensure they lead to the same value.

In this case, to minimalize this summation leads to:

$$k_1 = 6.9E-02\ \left[\frac{L}{g \cdot h}\right]$$

$$k_7 = 4.8\mathrm{E}-03\ \left[\frac{L}{g \cdot h}\right]$$

Which derive to the following fructose de rate values:

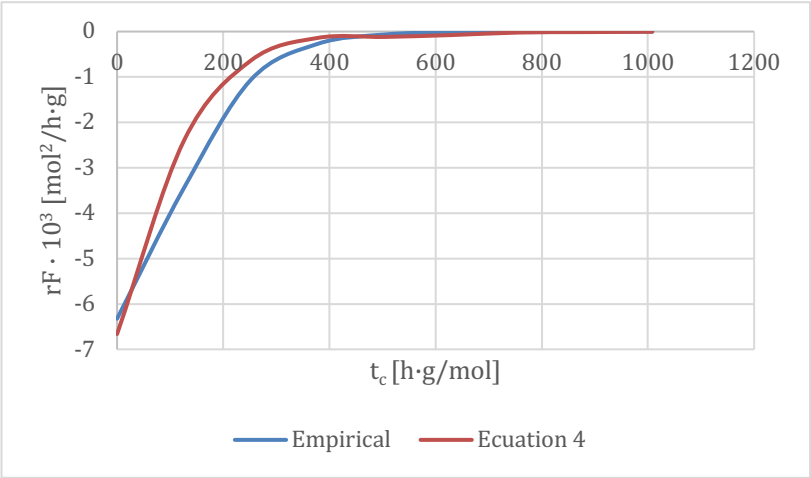

Figure 14. Reaction rate on fructose in the 1st experiment by different ways. Dowex 50Wx2, 120ºC, 1 g catalyst.

Figure 14 demonstrates that these calculated values of the kinetic constants lead to similar reaction rates as the estimated.

Kinetic constant units depend on the reaction order. This reaction order is the sum of the partial reaction order, which is regard to every compound. In this case, they have been obtained following equation 4, which shows:

$$\left[\frac{mol}{g \cdot h}\right] = k \cdot \left[\frac{mol}{L}\right]$$

And, in consequence, k units (for this case) are:

$$\left[\frac{L}{g \cdot h}\right]$$

For other kinetic constants these units change, but the procedure to obtain them has been the same.

Some of the kinetic constants appear in more than one compound rate, so it is necessary to make sure that all of them lead to a similar value. With the accuracy from which the data is based, it has been established that one kinetic constant obtained by reaction rates from different compounds must be, at least, of the same order of magnitude. Once this is achieved, is taken the average value as the one for that kinetic constant in that experiment (and consequently, temperature).

Kinetic constants depend on the temperature, so for those experiments made at same temperature (1st, 6th, 7th and 8th, 120ºC), they must be equals. The followed criteria is the same as before, kinetic constants must be of the same order of magnitude and then the average value is taken as the definitive. The obtained ones for each temperature are showed below:

120 ºC			
$\mathbf{k_1}$	6.9E-02 [L/(g·h)]	Least squares	
$\mathbf{k_2}$	1.9E-03 [L^2/(g·h·mol)]	r_F	1.5E-07
$\mathbf{k_3}$	1.7E-03 [L^2/(g·h·mol)]	r_{HMF}	2.7E-06
$\mathbf{k_4}$	4.7E-04 [L^2/(g·h·mol)]	r_{LA}	1.9E-07
$\mathbf{k_5}$	2.9E-03 [L^2/(g·h·mol)]	r_{BL}	5.3E-07
$\mathbf{k_6}$	4.0E-04 [L^2/(g·h·mol)]	r_{BMF}	1.0E-06
$\mathbf{k_7}$	4.8E-03 [L/(g·h)]	r_{FA}	5.9E-07
$\mathbf{k_8}$	5.1E-04 [L/(g·h)]	r_{BF}	6.9E-07

Table 4. Kinetic constants at 120ºC with the least squares values they imply.

110 ºC			
k_1	7.0E-02 [L/(g·h)]	Least squares	
k_2	4.9E-04 [L^2/(g·h·mol)]	r_F	5.5E-05
k_3	1.2E-03 [L^2/(g·h·mol)]	r_{HMF}	3.6E-07
k_4	4.9E-04 [L^2/(g·h·mol)]	r_{LA}	2.4E-06
k_5	2.8E-04 [L^2/(g·h·mol)]	r_{BL}	1.5E-07
k_6	8.3E-04 [L^2/(g·h·mol)]	r_{BMF}	7.0E-07
k_7	4.3E-03 [L/(g·h)]	r_{FA}	1.2E-07
k_8	4.0E-04 [L/(g·h)]	r_{BF}	2.7E-07

Table 5. Kinetic constants at 110ºC with the least squares values they imply.

100 ºC			
k_1	5.5E-02 [L/(g·h)]	Least squares	
k_2	7.5E-04 [L^2/(g·h·mol)]	r_F	1.1E-06
k_3	3.1E-04 [L^2/(g·h·mol)]	r_{HMF}	2.2E-07
k_4	8.7E-04 [L^2/(g·h·mol)]	r_{LA}	1.7E-08
k_5	4.1E-04 [L^2/(g·h·mol)]	r_{BL}	2.9E-07
k_6	1.2E-04 [L^2/(g·h·mol)]	r_{BMF}	1.8E-08
k_7	4.4E-03 [L/(g·h)]	r_{FA}	4.4E-08
k_8	2.9E-04 [L/(g·h)]	r_{BF}	8.6E-08

Table 6. Kinetic constants at 100ºC with the least squares values they imply.

90 ºC			
k_1	7.5E-03 [L/(g·h)]	Least squares	
k_2	1.3E-04 [L^2/(g·h·mol)]	r_F	1.4E-08
k_3	1.7E-04 [L^2/(g·h·mol)]	r_{HMF}	6.4E-07
k_4	-	r_{LA}	2.5E-08
k_5	8.6E-04 [L^2/(g·h·mol)]	r_{BL}	-
k_6	1.7E-04 [L^2/(g·h·mol)]	r_{BMF}	-
k_7	3.8E-03 [L/(g·h)]	r_{FA}	3.8E-10
k_8	2.2E-04 [L/(g·h)]	r_{BF}	-

Table 7. Kinetic constants at 90ºC with the least squares values they imply.

80 ºC			
k_1	3.9E-03 [(L·mol_{F^o})/(g·h)]	Least squares	
k_2	1.4E-05 [(L/· mol_{F^o})/(g·h·mol)]	r_F	1.0E-09
k_3	2.3E-04 [(L/· mol_{F^o})/(g·h·mol)]	r_{HMF}	1.7E-07
k_4	-	r_{LA}	4.6E-10
k_5	1.3E-03 [(L/· mol_{F^o})/(g·h·mol)]	r_{BL}	-
k_6	3.4E-04[(L/· mol_{F^o})/(g·h·mol)]	r_{BMF}	-
k_7	2.6E-03 [(L·mol_{F^o})/(g·h)]	r_{FA}	6.5E-10
k_8	1.7E-04 [(L·mol_{F^o})/(g·h)]	r_{BF}	-

Table 8. Kinetic constants at 80ºC with the least squares values they imply.

At 120ºC, the obtention of these constants have been made as explained above, one by one for each experiment and then taking the average value for every constant. This can be done because kinetic constants depend exclusively on the temperature. The least squares value shown is also an average of those experiments.

Note that HMF is usually the compound with a higher least squares value. That makes sense bearing in mind that the curve that presents its mole variation is not completely defined in most of experiments, as mentioned before, and this hinders the rate of formation estimation.

As expected, kinetic constants decrease as it does temperature. That is explained by thermal agitation; that says that a higher temperature implies more agitation of the molecules, which increase the probability of colliding between molecules and then the probability of having effective collides, which results in faster reactions. Since kinetic constants are the relation between the composition and the reaction rate, their value must increase as it does reaction rate (for direct reactions).

4.3 - KINETIC CHARACTERIZATION

As mentioned, kinetic constants exclusively depend on the temperature, but not on any other parameter of the reaction (catalyst presence, composition, …). This dependence is showed in Arrhenius Equation (12):

$$k = Ae^{\frac{-Ea}{RT}} \qquad (12)$$

This equation is constituted by:

- Preexponential factor (A): It is also characteristic of each reaction but it does not depend on temperature. The units are the same of the kinetic constant, explained previously.
- Activation energy (Ea): is considered the energetic barrier that reactants must overcome to become into products. It does not depend on the temperature. Is expressed in [kJ/mol].
- Temperature, expressed in [K]

Since A and Ea are constants, having the kinetic constant at different temperatures allow to calculate easily these two parameters. Applying logarithmic properties on equation (12) is obtained:

$$ln(k) = \ln(A) - \frac{Ea}{R}\left(\frac{1}{T}\right) \quad (13)$$

Where R represents the ideal gas constant (8.314 J/(mol·K))

This equation shows a linear dependence of (1/T) versus ln(k), since it has the same form as a linear equation (equation (14)).

$$y = mx + n \quad (14)$$

Being the activation energy obtained by the slope of the curve and the preexponential factor by the y-intercept. This allows making a linear regression to obtain the sought parameters, with ln(k) and the (1/T) the dependent and independent variables, respectively.

Ideally, the five obtained constant at different temperatures lead to a perfect linear regression of ln(k) versus (1/T), as seen in equation (13). The reality is that the reaction was performed under such dilute conditions that the concentrations were in the limit of the chromatograph's readability, which gives rise to an experimental inaccuracy that is reflected in the obtained results. In addition, this is a preliminary model and is not as accurate as it can be a more complex model without the assumptions implied.

The regressions made have been:

A

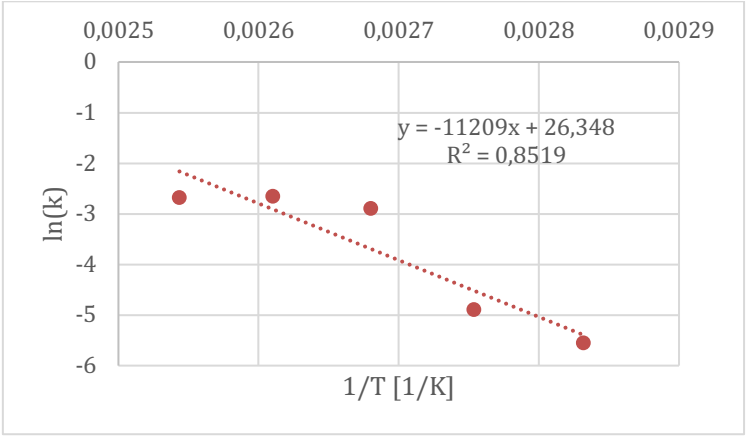
0,0025
0,0026
0,0027
0,0028
0,0029
0
-1
-2
-3
-4
-5
-6
ln(k)
y = -11209x + 26,348
R² = 0,8519
1/T [1/K]

B

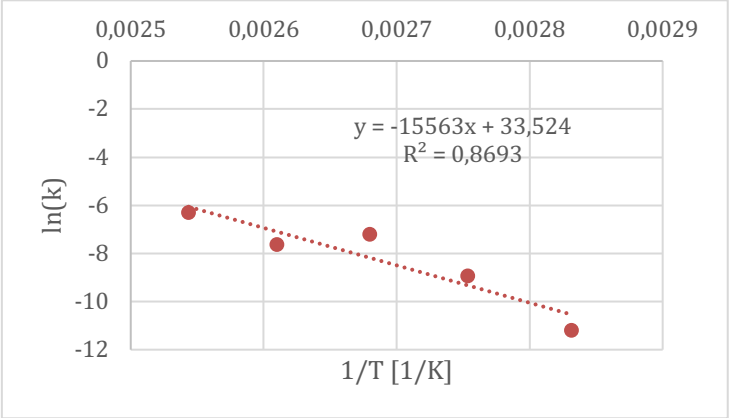
0,0025
0,0026
0,0027
0,0028
0,0029
0
-2
-4
-6
-8
-10
-12
ln(k)
y = -15563x + 33,524
R² = 0,8693
1/T [1/K]

C

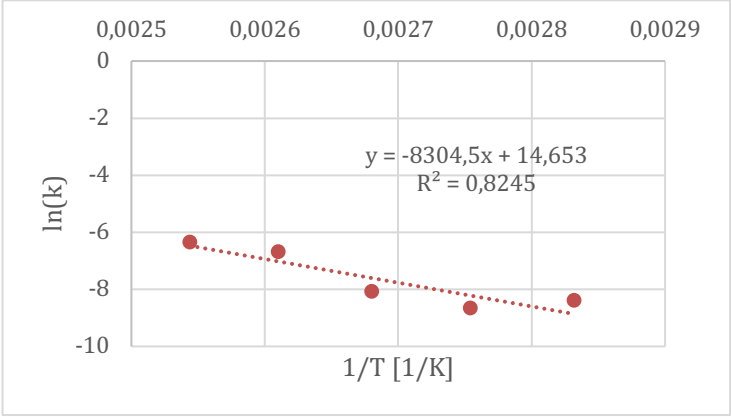
0,0025
0,0026
0,0027
0,0028
0,0029
0
-2
-4
-6
-8
-10
ln(k)
y = -8304,5x + 14,653
R² = 0,8245
1/T [1/K]

D

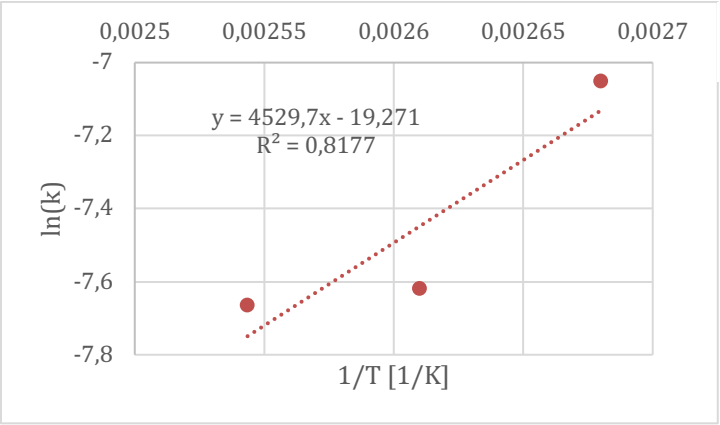
0,0025
0,00255
0,0026
0,00265
0,0027
-7
-7,2
-7,4
-7,6
-7,8
ln(k)
y = 4529,7x - 19,271
R² = 0,8177
1/T [1/K]

E

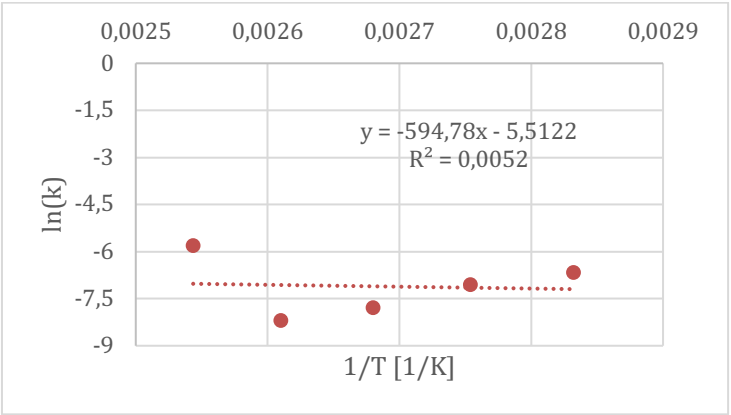
0,0025
0,0026
0,0027
0,0028
0,0029
0
-1,5
-3
-4,5
-6
-7,5
-9
ln(k)
y = -594,78x - 5,5122
R² = 0,0052
1/T [1/K]

F

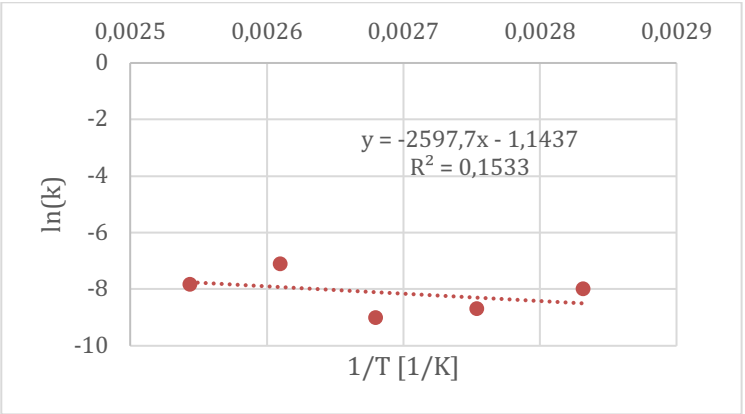
0,0025
0,0026
0,0027
0,0028
0,0029
0
-2
-4
-6
-8
-10
ln(k)
y = -2597,7x - 1,1437
R² = 0,1533
1/T [1/K]

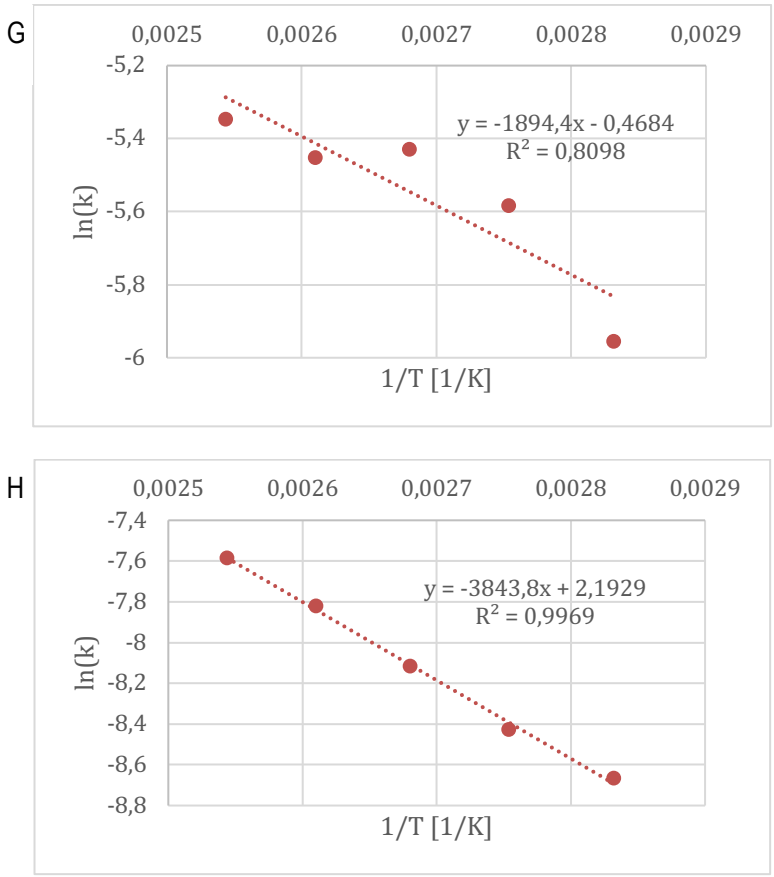

Figure 15. Representation of equation 13 for A: k_1, B: k_2, C: k_3, D: k_4, E: k_5, F: k_6, G: k_7, H: k_8.

Because of the lack of data of some compounds at lower temperatures, k_4 just had value for 120, 110 and 100ºC. Figure 15-D shows how kinetic constants decrease as temperature increases. According with thermal agitation, mentioned before, this makes no physical sense, so this regression cannot be considered. This can be because k_4 related the transformation of BMF to BL and BF, which are the three compounds with lower values of moles, and that leads to a higher inaccuracy of the chromatograph as mentioned before.

It is also worth mentioning Figure 15-E, where the slope of the regression is practically zero. This is because the sensitivity of the kinetic constant with the temperature is extremely low. In Figure 15-D, this sensibility is also low but not as much as in the first case. The lack of sensitivity implies that the effect of the temperature on the kinetic constant is not very remarkable.

For the rest of the experiments, the linear regression is not mathematically accurate, but they generally lead to acceptable values, thermodynamically coherents. This can be considered a success bearing in mind the sum of the experimental inaccuracy of the chromatograph and the inaccuracy derived from the assumptions made for a pseudo-homogeneous model.

The parameters obtained by Figure 15 can be seen in Table 9:

	Ea [kJ/mol]	**A**
(A) k_1	93 ± 22	2.8E+11 $\pm$ 1.3E+03 [(L)/(g·h)]
(B) k_2	129 ± 29	3.6E+14 $\pm$ 1.0E+04[(L^2/(g·h·mol)]
(C) k_3	69 ± 18	2.3 E+06 $\pm$ 3.9E+02 [(L^2/(g·h·mol)]
(D) k_4	-	-
(E) k_5	5 ± 39	4.0E-03 $\pm$ 3E+05 [(L^2/(g·h·mol)]
(F) k_6	22 ± 29	3.2E-01 $\pm$ 1.4E+04 [(L^2/(g·h·mol)]
(G) k_7	16 ± 4	1.6 $\pm$ 4.2 [(L)/(g·h)]
(H) k_8	32 ± 0.1	8.9 $\pm$ 1.4[(L)/(g·h)]

Table 9. Obtained Ea and A for each kinetic constant.

Note that the activation energy for reactions 5 and 6, the confidence interval includes the zero, which is not thermodynamically possible. In all reactions, no matter how low can be, reactants need to overcome the activation energy, even in spontaneous reactions, so activation energy cannot be zero.

These reactions define the esterification of LA and FA to BL and BF, respectively. Once again are seen the consequences of such low concentrations of the involved compounds.

4.4 - APPROXIMATION OF THE HUMINS FORMATION

Knowing all the kinetic constants and concentrations let the calculation of humins rate, which can explain the behavior deviation of some experiments. Following the scheme of the reaction (Figure 13) and the pseudo-homogeneous model we arrive at:

$$r_{humins} = r_7 + r_8 = k_7 \cdot c_F + k_8 \cdot c_{HMF} \quad (15)$$

It is important to remark that this is a calculation with obtained values after some calculation done with experimental data. This means that these values are not accurate enough to determine the humins reaction rate as it is, but it can give an idea of their formation for each experiment.

The obtained reaction rates are:

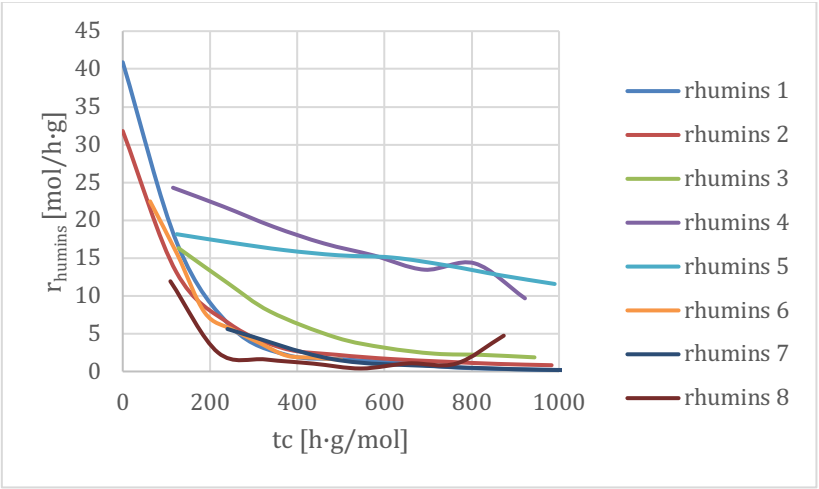

Figure 16. Humins reaction rate for all experiments (1st – 8th).

Figure 16 shows a clearly difference between experiments 4 (90ºC) and 5 (80ºC) and the rest of experiments (100-120ºC). This is in concordance of the mentioned in introduction, that lower temperatures favour side reactions. As said, humins formation is the main determinant of reaction yield, so it makes sense that precisely those experiments with higher formation of humins are the ones with such low decomposition rates of fructose (as the main reagent) that led to a low content of product, such that it is not even detected in the chromatograph.

Although, it would require more data and a deeper study to determine more accurately this humins formation and their consequences.

5. CONCLUSIONS

It is proposed a pseudo-homogeneous model as a preliminary study of the kinetics of the obtention of butyl levulinate from fructose and 1-butanol. This study is made from experiments between 80 and 120ºC and uses very diluted mixtures of fructose in the initial mixture (water-butanol), what leads to low concentrations of some compounds and in consequence, complicates the estimation of the rate of formation.

Also, the reaction medium has been considered ideal, and concentrations have been used instead of activities for the reaction rate calculation. However, the proposed model can be considered satisfactory since it describes properly the experimental data.

Activation energies found by Arrhenius equation are thermodynamically coherent for all reactions except for the formation of butyl levulinic and butyl formate from BMF. Which can be explained by the dilute conditions, that led to low changes in the reaction rate.

Humins formation has been estimated following the pseudo-homogeneous model and their formation is in agreement with literature.

The next step for this kinetic study to which this one contributes, would be to find the definitive model, not considering ideality and using a heterogeneous model to describe the reaction. Although this requires more experimental data.

6. REFERENCES AND NOTES

[1] NIGAM, P.S. y SINGH, A., 2011. Production of liquid biofuels from renewable resources. Progress in energy and combustion science, **37**, 52-68. DOI 10.1016/j.pecs.2010.01.003.

[2] Jeswani HK, Chilvers A, Azapagic A. 2020 Environmental sustainability of biofuels: a review. Proc. R. Soc. A **476**: 20200351.

[3] REGALBUTO, J.R., 2009. Cellulosic Biofuels: Got Gasoline? Science (American Association for the Advancement of Science), **325**, no. 5942. DOI 10.1126/science.1174581.

[4] DI MENNO DI BUCCHIANICO, D., MIGNOT, M., BUVAT, J.-C., CASSON MORENO, V. y LEVENEUR, S., 2023. Production of butyl levulinate from the solvolysis of high-gravity fructose over heterogeneous catalyst: In-depth kinetic modeling. Chemical engineering journal (Lausanne, Switzerland : 1996), **465**. DOI 10.1016/j.cej.2023.142914.

[5] CLARK, J.H. y DESWARTE, F., 2014. Pretreatment and Thermochemical and Biological Processing of Biomass. Introduction to Chemicals from Biomass. United Kingdom: Wiley, pp. 53-88. ISBN 1118714482.

[6] MOTA, C.J.A et al., 2023. Levulinic acid: a sustainable platform chemical for value-added products. Hoboken, New Jersey: John Wiley & Sons, Incorporated. ISBN 1-119-81471-5.

[7] FERNANDES, D.R., ROCHA, A.S., MAI, E.F., MOTA, C.J.A. y TEIXEIRA DA SILVA, V., 2012. Levulinic acid esterification with ethanol to ethyl levulinate production over solid acid catalysts. Applied catalysis. A, General, **425-426**,199-204. DOI 10.1016/j.apcata.2012.03.020.

[8] DÉMOLIS, A., ESSAYEM, N. y RATABOUL, F., 2014. Synthesis and Applications of Alkyl Levulinates. ACS sustainable chemistry & engineering, **2**, no. 6. DOI 10.1021/sc500082n.

[9] JOSHI, H., MOSER, B.R., TOLER, J., SMITH, W.F. y WALKER, T., 2011. Ethyl levulinate: A potential bio-based diluent for biodiesel which improves cold flow properties. Biomass & bioenergy, **35**, no. 7,3262-3266. DOI 10.1016/j.biombioe.2011.04.020.

[10] TEJERO IBORRA, M.À., 2015. A contribution to the study of butyl levulinate synthesis in the liquid-phase on ion-exchange resins. S.l.: s.n.

[11] RAMÍREZ, E., BRINGUÉ, R., FITÉ, C., IBORRA, M., TEJERO, J. y CUNILL, F., 2021. Assessment of ion exchange resins as catalysts for the direct transformation of fructose into butyl levulinate. Applied catalysis. A, General, **612**. DOI 10.1016/j.apcata.2021.117988.

[12] CORAIN, B., ZECCA, M. y JERABEK, K., 2001. Catalysis and polymer networks: the role of morphology and molecular accessibility: Catalysis inside functional synthetic resins: the issue of catalyst access ibility and stability. Journal of molecular catalysis. A, Chemical, **177**, no. 1, 3-20.

[13] IZQUIERDO, J.F.,CUNILL, F., TEJERO, J., IBORRA, M. Y FITÉ, C. 2004. Cinética de las reacciones químicas. Barcelona: Edicions Universitat de Barcelona. ISBN 8483384795.

[14] RAMÍREZ RANGEL, E., BRINGUE TOMÁS, R., FITÉ PIQUER, C., IBORRA URIOS, M., TEJERO SALVADOR, X. y CUNILL GARCÍA, F., 2017. Role of ion-exchange resins as catalysts in the reaction-network of transformation of biomass into biofuels. Journal of chemical technology and biotechnology (1986), **92**, 2775-2786.

[15] ARESTA, M. (Michele), DIBENEDETTO, A. y DUMEIGNIL, F., 2012. Biorefinery from biomass to chemicals and fuels. 1st ed. Berlin ; Walter de Gruyter. ISBN 1-68015-208-4.

[16] CLIMENT, M.J., CORMA, A. y IBORRA, S., 2014. Conversion of biomass platform molecules into fuel additives and liquid hydrocarbon fuels. Green chemistry : an international journal and green chemistry resource : GC, **16**, no. 2, 516-547. DOI 10.1039/c3gc41492b.

[17] AELLIG, C. y HERMANS, I., 2012. Continuous D-Fructose Dehydration to 5- Hydroxymethylfurfural Under Mild Conditions. ChemSusChem, **5**, no. 9,1737-1742. DOI 10.1002/cssc.201200279.

[18] SHARMA, R., 2016. A contribution to the study of acidic ion-exchange resins to produce butyl levulinate from fructose and butyl alcohol. S.l.: s.n.

[19] IBORRA URIOS, M., TEJERO SALVADOR, J., FITÉ PIQUER, C., RAMÍREZ RANGEL, E. y CUNILL GARCÍA, F., 2019. Liquid-phase synthesis of butyl levulinate with simultaneous water removal catalyzed by ion exchange resins.

[20] YOU, Z., YU, M., FU, R., NIE, X. y CHEN, J., 2024. Synthesis and Properties of a Novel Levulinic Acid-Based Environmental Auxiliary Plasticizer for Poly(vinyl chloride). Polymers, **16**, no. 3, 361. DOI 10.3390/polym16030361.

7. ACRONYMS

F fructose.

HMF 5-hydroxymetil furfural.

LA levulinic acid.

FA formic acid.

BMF 5-hydroxybutil furfural.

BL butyl levulinate.

BF butyl formate.

AL alkyl levulinate.

$\mathbf{n_j}$ mole of species j, mol.

$\mathbf{r_j}$ rate of formation of species j, mol_j /(g·h).

$\mathbf{t_c}$ contact time, (h·g)/mol.

t time, h.

W catalyst mass, g.

$\mathbf{n_{F^o}}$ initial mole of fructose, mol_F.

k kinetic constant, L/(g·h), L^2/(g·h·mol).

Ea activation energy.

A preexponential factor, L/(g·h), L^2/(g·h·mol).

DVB Divinylbenzene.

$\mathbf{d_p}$ particle diameter, mm.

$\mathbf{d_{pore}}$ (macro) pore diameter, mm.

$\mathbf{T_{max}}$ maximum work temperature, ºC.

$\mathbf{V_{pore}}$ global (macro) pore volume cm^3/g.

$\mathbf{s_{pore}}$ global (macro) pore surface, m^2/g.

$\mathbf{V_{sp}^e}$ specific volume of swollen polymer, cm^3/g.

Capítulo 1 APPENDICES

APPENDIX 1: EMPIRICAL MODEL EQUATIONS

Ratkowsky	$\boldsymbol{n = \frac{a}{1 + e^{b - ct_c}}}$
Modified power	$n = ab^{t_c}$
Rational	$n = \frac{a + bt_c}{1 + ct_c + dt_c{}^3}$
Exponential	$n = ae^{bt_c}$
Logistic	$n = \frac{a}{1 + be^{-ct_c}}$
Bleasdale	$n = (a + bt_c)^{-\frac{1}{c}}$
Exponential association 2	$n = a(1 - e^{-bt_c})$
Modified hoerl	$n = ab^{\left(\frac{1}{t_c}\right)}t_c{}^c$
Dr-hill zero background	$n = \frac{\theta t_c{}^\eta}{\kappa^\eta + t_c{}^\eta}$
Dr-hill	$n = \propto + \frac{\theta t_c{}^\eta}{\kappa^\eta + t_c{}^\eta}$
Steinhart-Hart	$n = \frac{1}{A + Bln(t_c) + Cln(t_c)^3}$
Heat capacity	$n = a + bt_c + \frac{c}{t_c{}^2}$
Power	$n = at_c{}^b$
Modified experimental	$n = ae^{\frac{b}{t_c}}$

Table 10. Empirical model equations

APPENDIX 2: USED EMPIRICAL MODELS FOR EVERY COMPOUND.

1st EXPERIMENT				
Dowex 50Wx2. 120ºC. 1 g cata				
Compound	**Model**	**Parameters**		**Least squares**
F	Ratkowsky	a	0.2E-02 ± 6E-02	1.64E+05
		b	2E-01 ± 7E-01	
		c	1.1E-02 ± 2E-03	
HMF	Polynomial (degree 7)	a	2E-06 ± 7E-04	2.80E+05
		b	6E-05 ± 6E-05	
		c	-4E-07 ± 9E-07	
		d	1E-09 ± 5E-09	
		e	-1E-12 ± 1E-11	
		f	-1E-15 ± 2E-14	
		g	-4-19 ± 1E-17	
		h	6E-23 ± 4E-21	
LA	Steinhart-Hart	A	1.1E+04 ± 5E+03	5.17E+05
		B	-2E+03 ± 1E+03	
		C	1E+01 ± 1E+01	

Compound	**Model**	**Parameters**		**Least squares**
BL	Rational	a	-2E-04 ± 4E-04	3,25E+05
		b	6E-06 ± 3E-06	
		c	1E-03 ± 2E-03	
		d	2E-08 ± 7E-07	
BMF	Rational	a	6E-05 ± 6E-04	1,85E+06
		b	6E-06 ± 5E-06	
		c	-4E-04 ± 2E-04	
		d	1.9E-06 ± 5E-07	
FA	Rational	a	-1E+04 ± 7E+10	3,62E+06
		b	1E+02 ± 1E+09	
		c	5E+04 ± 4E+11	
		d	-3E+00 ± 2E+07	
BF	Rational	a	-9E-04 ± 2E-03	9,74E+08
		b	1E-05 ± 2E-05	
		c	7-03 ± 1E-02	
		d	-1E-06 ± 4E-06	

Table 11. Kinetic fit models for 1st experiment.

2nd EXPERIMENT				
Dowex 50Wx2, 110ºC, 1 g cata				
Compound	**Model**	**Parameters**		**Least squares**
F	Modified power	a	7.45E-03 ± 6E-05	1.52E+14
		b	9.916E-01 ± 2E-04	
HMF	Polinomial (degree 6)	a	6E-04 ± 6E-04	4.25E+14
		b	5E-05 ± 3E-05	
		c	-2E-07 ± 3E-07	
		d	5E-10 ± 1E-09	
		e	-6E-13 ± 2E-12	
		f	3E-16 ± 2E-15	
		g	-9E-20 ± 7E-19	
LA	Rational	a	1E-04 ± 1E-04	9.71E+14
		b	6E-06 ± 8E-06	
		c	8E-03 ± 2E-02	
		d	-8E-07 ± 6E-06	

Compound	**Model**	**Parameters**		**Least squares**
BL	Steinhart-Hart	A	1E+04 ± 1E+04	2.47E+14
		B	-2E+03 ± 3E+03	
		C	5 ± 3E+01	
BMF	Dr Hill zero background	theta	4E-03 ± 2E-03	5.34E+14
		eta	1.2 ± 2E-01	
		kappa	9E+02 ± 5E+02	
FA	Dr Hill zero background	theta	4E-03 ± 6E-03	2.20E+14
		eta	8E-01 ± 1	
		kappa	6E+02 ± 3E+04	
BF	Exponential association 2	a	2E-03 ± 1E-01	1.13E+14
		b	1.1E-03 ± 7E-04	

Table 12. Kinetic fit models for 2nd experiment.

3rd EXPERIMENT				
Dowex 50Wx2, 100ºC, 1 g cata				
Compound	**Model**	**Parameters**		**Least squares**
F	Rational	a	7.8E+03 ± 4E-04	1.03E+07
		b	-8E-06 ± 3E+06	
		c	6E-03 ± 2E-03	
		d	5E-06 ± 2E-05	
HMF	Rational	a	-1E-03 ± 3E-03	6.32E+06
		b	3E-05 ± 3E-05	
		c	3E-04 ± 3E-03	
		d	6E-06 ± 3E-06	
LA	Dr hill zero background	theta	9.8E-04 ± 2E-03	5.30E+05
		eta	1E+00 ± 1E+00	
		kappa	7E+03 ± 2E+04	
BL	Steinhart-Hart	A	4.9E+04 ± 9E+03	2.78E+03
		B	-1.0E+04 ± 2E+03	
		C	6E+01 ± 2E+01	

Compound	**Model**	**Parameters**		**Least squares**
BMF	Dr hill	alpha	3E-04 ± 2E-04	3.33E+04
		thet	1.7E-03 ± 9E-04	
		eta	3E+00 ± 2E+00	
		kappa	8E+02 ± 2E+02	
FA	Rational	a	8E-05 ± 4E-04	8.59E+06
		b	5E-07 ± 1E-06	
		c	-2E-03 ± 2E-03	
		d	8E-07 ± 1E-06	
BF	Rational (a)	a	-8,01E+07	1.16E+06
		b	1.36E+03	
		c	-2,56E+06	
		d	8.89E-01	

(a)There were not enough values of this compound to determine the confidence interval.

Table 13. Kinetic fit models for 3rd experiment.

4th EXPERIMENT			
Dowex 50Wx2, 90ºC, 1 g cata			
Compound	**Model**	**Parameters**	**Least squares**
F	Exponential	a 7,5E-03 ± 5E-04 b -1.2E-03 ± 2E-04	5.15E-07
HMF	Rational	a -1E-03 ± 2E-03 b 2E-05 ± 2E-05 c 3E-03 ± 4E-03 d -7E-07 ± 2E-06	3.15E-08
LA	Rational	a -2E+02 ± 3E+09 b 3E+00 ± 9E+07 c 1E+04 ± 4E+11 d -4E+00 ± 1E+08	1.23E-09
BL	-		
BMF	-		
FA	Power	a 6E-10 ± 3E-09 b 1.9E+00 ± 9E-01	5.03E-09
BF	-		

Table 14. Kinetic fit models for 4th experiment.

5th EXPERIMENT				
Dowex 50Wx2. 80ºC. 1 g cata				
Compound	**Model**	**Parameters**		**Least squares**
F	Exponential	a b	7.6E-03 ± 3E-04 -5.3E-04 ± 7E-05	2.00E+07
HMF	Exponential association 2	a b	1E-01 ± 2E+00 2E-05 ± 3E-04	4.83E+06
LA	Steinhart-Hart	A B C	-1E+04 ± 2E+04 6E+03 ± 5E+03 -6E+01 ± 5E+01	4.23E+04
BL	-			
BMF	-			
FA	Dr hill zero background	theta eta kappa	1E-04 ± 1E-04 5E+00 ± 2E+00 1.0E+04 ± 4E+03	2.41E+02
BF	-			

Table 15. Kinetic fit models for 5th experiment.

6th EXPERIMENT			
Dowex 50Wx2, 120ºC, 0,5 g cata			
Compound	**Model**	**Parameters**	**Least squares**
F	Logistic	a -9E-02 ± 5E-01 b -1E+01 ± 6E+01 c -9E-03 ± 3E-03	1.21E-07
HMF	Modified hoerl	a 3E+01 ± 6E+01 b 4E-96 ± 2E-94 c -1.5E+00 ± 3E-01	1.61E-07
LA	Modified hoerl	a 7E-04 ± 1E-03 b 3E-40 ± 1E-38 c 3E-02 ± 2E-01	2.85E-09
BL	Power	a 8E-06 ± 5E-06 b 9E-01 ± 1E-01	9.43E-09
BMF	Dr hill zero background	theta 4E-03 ± 2E-03 eta 1,2E+00 ± 4E-01 kappa 3E+02 ± 3E+02	1.86E-08
FA	Richards	a 2,9E-03 ± 2E-04 b -6E-01 ± 1E+00 c 1,2E-02 ± 9E-03 d 1E-01 ± 2E+00	1.74E-08
BF	Dr hill zero background	theta 2E-03 ± 1E-03 eta 1,5E+00 ± 7E-01 kappa 3E+02 ± 2E+02	5.91E-09

Table 16. Kinetic fit models for 6th experiment.

7th EXPERIMENT				
Dowex 50Wx2, 120ºC, 2 g cata				
Compound	**Model**	**Parameters**		**Least squares**
F	Bleasdale	a	2.2E+00 ± 1E-01	4.29E-11
		b	4.5E-03 ± 7E-04	
		c	1.7E-01 ± 1E-02	
HMF	Dr hill zero background	theta	3.8E-03 ± 6E-04	3.17E-08
		eta	-2.6E+00 ± 6E-01	
		kappa	4.4E+02 ± 9E+01	
LA	Dr hill zero background	theta	6E-03 ± 4E-02	3.28E-09
		eta	4E-01 ± 5E-01	
		kappa	8E+04 ± 2E+06	

Compound	**Model**	**Parameters**		**Least squares**
BL	Steinhart-hart	A	5E+03 ± 2E+03	7,30E-08
		B	-9E+02 ± 5E+02	
		C	5E+00 ± 4E+00	
BMF	Rational	a	7E-04 ± 7E-04	1.41E-08
		b	4E-06 ± 4E-06	
		c	-3E-04 ± 7E-04	
		d	1.1E-06 ± 5E-07	
FA	Steinhart-hart	A	2E+03 ± 1E+03	1.27E-07
		B	-2E+02 ± 3E+02	
		C	1E+00 ± 2E+00	
BF	Modified exponential	a	3E-03 ± 4-04	1.23E-07
		b	-3.5E+02 ± 9E+01	

Table 17. Kinetic fit models for 7th experiment.

8th EXPERIMENT			
Dowex 50Wx2. 120ºC. 1g cata			
Compound	**Model**	**Parameters**	**Least squares**
F	Exponential	a 9E-03 ± 1E-03 b -1.4E-02 ± 4E-03	9,80E+07
HMF	Rational	a 6E-04 ± 1E-03 b 1E+03 ± 2E+10 c 7E+02 ± 1E+10 d 1E+03 ± 2E+10	9,80E+07
LA	Heat capacity	a 4E-04 ± 2E-04 b 7E-07 ± 2E-07 c -2E+00 ± 2E+00	1,03E+06
BL	Rational	a -3E-05 ± 4E-04 b 1E-05 ± 1E-05 c 6E-03 ± 1E-02 d -5E-06 ± 8E-06	1,34E+07
BMF	Rational	a -9E-06 ± 4E-04 b 1.6E-05 ± 6E-06 c -2E-03 ± 1E-03 d 1.0E-05 ± 2E-06	9,93E+06
FA	Heat capacity	a 1E-03 ± 2E-03 b 3E-06 ± 3E-06 c -6E+00 ± 3E+01	1,60E+08
BF	Rational	a -2E-03 ± 9E-03 b 4E-05 ± 2E-04 c 2E-02 ± 9E-02 d -1E-05 ± 5E-05	1,19E+06

Table 18. Kinetic fit models for 8th experiment.

APPENDIX 3: CONCENTRATIONS OF ALL COMPOUNDS THROUGH TIME.

Dowex 50Wx2, 120ºC, 1 g cata

t [h]	t_c [h·g/mol]	C_F [mol/L]	C_{HMF} [mol/L]	C_{LA} [mol/L]	C_{BL} [mol/L]	C_{BMF} [mol/L]	C_{FA} [mol/L]	C_{BF} [mol/L]	C_{BuOH} [mol/L]	C_{H2O} [mol/L]
0	0	0,1038	0,0000						8,4223	7,5631
1	126,03	0,0374	0,0501	0,0056	0,0067	0,0108	0,0193	0,0069	8,4186	7,3438
2	252,05	0,0099	0,0450	0,0082	0,0137	0,0213	0,0320	0,0137	8,4148	7,2190
3	378,08	0,0022	0,0323	0,0092	0,0195	0,0277	0,0347	0,0188	8,4066	7,1911
4	504,11	0,0018	0,0222	0,0096	0,0239	0,0324	0,0355	0,0213	8,4343	7,0433
5	630,13	0,0012	0,0166	0,0106	0,0270	0,0349	0,0380	0,0231	8,4618	6,9306
6	756,16	0,0003	0,0104	0,0109	0,0311	0,0349	0,0391	0,0250	8,4977	6,7642
7	882,12	0,0002	0,0061	0,0117	0,0330	0,0357	0,0416	0,0261	8,4713	6,8395
8	1008,21	0,0001	0,0042	0,0107	0,0353	0,0321	0,0399	0,0284	8,4575	6,8912

Table 19. Concentrations through time for the 1st experiment.

Dowex 50Wx2, 110ºC, 1 g cata

t [h]	t_c [h·g/mol]	C_F [mol]	C_{HMF} [mol]	C_{LA} [mol]	C_{BL} [mol]	C_{BMF} [mol]	C_{FA} [mol]	C_{BF} [mol]	C_{BuOH} [mol]	C_{H2O} [mol]
0	0	0,099	0,008	0,002			0,001		8,711	6,901
1	122,88	0,036	0,061	0,006		0,005	0,015		8,688	6,817
2	245,76	0,013	0,072	0,008	0,006	0,010	0,016		8,566	7,191
3	368,64	0,004	0,063	0,008	0,010	0,015	0,024	0,010	8,493	7,342
4	491,52	0,002	0,057	0,008	0,013	0,019	0,029	0,013	8,527	7,186
5	614,4	0,001	0,046	0,008	0,017	0,024	0,029	0,015	8,550	7,108
6	737,28	0,001	0,038	0,010	0,018	0,027	0,036	0,016	8,528	7,186
7	860,16	0,000	0,032	0,009	0,024	0,029	0,032	0,019	8,563	7,015
8	983,04	0,000	0,027	0,010	0,032	0,032	0,035	0,020	8,597	6,824

Table 20. Concentrations through time for the 2nd experiment.

Dowex 50Wx2, 100ºC, 1 g cata

t [h]	t_c [h·g/mol]	C_F [mol/L]	C_{HMF} [mol/L]	C_{LA} [mol/L]	C_{BL} [mol/L]	C_{BMF} [mol/L]	C_{FA} [mol/L]	C_{BF} [mol/L]	C_{BuOH} [mol/L]	C_{H2O} [mol/L]
0,00	0	0,104							8,863	6,735
1,08	127,81	0,048	0,035	0,002			0,001		8,846	6,729
2,03	239,89	0,031	0,064	0,004			0,006		8,743	7,005
2,87	338,2	0,019	0,077	0,004		0,006	0,006		8,657	7,176
4,13	487,64	0,008	0,079	0,005	0,006	0,009	0,011		8,655	7,168
5,10	601,69	0,004	0,077	0,006	0,008	0,012	0,012	0,001	8,642	7,210
6,07	715,73	0,002	0,073	0,007	0,010	0,014	0,021	0,009	8,696	6,996
7,00	825,84	0,002	0,070	0,007	0,013	0,017	0,023	0,010	8,709	6,872
8,00	943,82	0,002	0,061	0,007	0,015	0,020	0,027	0,012	8,650	7,053

Table 21. Concentrations through time for the 3rd experiment.

Dowex 50Wx2, 90ºC, 1 g cata

t [h]	t_c [h·g/mol]	C_F [mol/L]	C_{HMF} [mol/L]	C_{LA} [mol/L]	C_{BL} [mol/L]	C_{BMF} [mol/L]	C_{FA} [mol/L]	C_{BF} [mol/L]	C_{BuOH} [mol/L]	C_{H2O} [mol/L]
0	0	0,106							8,593	6,983
1	115,24	0,088	0,013	0,002					8,568	7,076
2	230,48	0,078	0,030	0,003			0,000		8,526	7,161
3	345,72	0,067	0,042	0,003			0,001		8,506	7,206
4,25	460,96	0,059	0,054	0,003			0,002		8,508	7,136
5	576,2	0,052	0,060	0,003			0,002		8,512	7,055
6	691,44	0,045	0,068	0,004			0,002		8,497	7,037
7	806,68	0,048	0,072	0,004		0,005	0,004		8,496	7,039
8	921,93	0,031	0,080	0,004		0,006	0,004		8,470	7,027

Table 22. Concentrations through time for the 4th experiment.

Dowex 50Wx2, 80ºC, 1 g cata

t [h]	t_c [h·g/mol]	C_F [mol/L]	C_{HMF} [mol/L]	C_{LA} [mol/L]	C_{BL} [mol/L]	C_{BMF} [mol/L]	C_{FA} [mol/L]	C_{BF} [mol/L]	C_{BuOH} [mol/L]	C_{H2O} [mol/L]
0	0	0,106							8,738	7,419
1	123,75	0,095	0,008	0,002					8,739	7,419
2	247,5	0,089	0,011	0,002					8,734	7,392
3	371,25	0,083	0,019	0,002					8,777	7,239
4	495,01	0,079	0,027	0,002			0,000		8,644	7,703
5	618,76	0,077	0,031	0,002			0,000		8,711	7,465
6	742,51	0,072	0,038	0,003			0,000		8,739	7,290
7	866,26	0,064	0,045	0,002			0,001		8,775	7,195
8	990,01	0,058	0,051	0,003			0,001		8,767	7,258

Table 23. Concentrations through time for the 5th experiment.

Dowex 50Wx2, 120ºC, 0,5 g cata

t [h]	t_c [h·g/mol]	C_F [mol/L]	C_{HMF} [mol/L]	C_{LA} [mol/L]	C_{BL} [mol/L]	C_{BMF} [mol/L]	C_{FA} [mol/L]	C_{BF} [mol/L]	C_{BuOH} [mol/L]	C_{H2O} [mol/L]
0	0	0,108							8,527	7,354
1	62,64	0,057	0,026	0,002		0,006	0,007		8,528	7,190
2	125,28	0,036	0,053	0,006	0,007	0,012	0,017	0,006	8,571	6,915
3	187,92	0,015	0,050	0,006	0,010	0,016	0,024	0,010	8,527	7,014
4	250,55	0,010	0,046	0,008	0,013	0,021	0,031	0,013	8,524	6,975
5	313,19	0,006	0,043	0,008	0,015	0,025	0,033	0,015	8,555	6,843
6	375,83	0,002	0,033	0,009	0,020	0,025	0,035	0,018	8,535	6,910
7	438,47	0,002	0,028	0,009	0,021	0,029	0,034	0,019	8,545	6,847
8	501,11	0,002	0,023	0,010	0,024	0,031	0,036	0,021	8,564	6,756

Table 24. Concentrations through time for the 6th experiment.

Dowex 50Wx2, 120ºC, 2 g cata

t [h]	t_c [h·g/mol]	C_F [mol/L]	C_{HMF} [mol/L]	C_{LA} [mol/L]	C_{BL} [mol/L]	C_{BMF} [mol/L]	C_{FA} [mol/L]	C_{BF} [mol/L]	C_{BuOH} [mol/L]	C_{H2O} [mol/L]
0	0	0,108							8,493	7,098
1	240,01	0,010	0,043	0,008	0,014	0,024	0,032	0,014	8,412	7,032
2	480,03	0,002	0,023	0,010	0,024	0,034	0,036	0,021	8,373	7,065
3	720,04	0,001	0,013	0,012	0,033	0,038	0,046	0,026	8,366	7,011
4	960,05	0,000	0,005	0,012	0,035	0,039	0,047	0,030	8,365	6,971
5	1200,07	0,000	0,003	0,013	0,039	0,035	0,047	0,034	8,348	6,998
6	1440,08	0,000	0,002	0,015	0,043	0,033	0,052	0,037	8,350	6,969
7	1680,09	0,000	0,002	0,015	0,045	0,029	0,053	0,039	8,354	6,948
8	1920,11	0,000	0,002	0,015	0,049	0,028	0,054	0,039	8,407	6,731

Table 25. Concentrations through time for the 7th experiment.

Dowex 50Wx2, 120ºC, 1g cata

t [h]	t_c [h·g/mol]	C_F [mol/L]	C_{HMF} [mol/L]	C_{LA} [mol/L]	C_{BL} [mol/L]	C_{BMF} [mol/L]	C_{FA} [mol/L]	C_{BF} [mol/L]	C_{BuOH} [mol/L]	C_{H2O} [mol/L]
0	0	0,123							9,253	5,188
1	109,23	0,026	0,097	0,004	0,009	0,028	0,012	0,013	9,290	4,710
2	218,45	0,003	0,042	0,007	0,018	0,053	0,019	0,020	9,308	4,465
3	327,68	0,001	0,036	0,008	0,024	0,055	0,034	0,026	9,297	4,397
4	436,91	0,001	0,025	0,009	0,027	0,052	0,027	0,029	9,326	4,262
5	546,14	0,000	0,011	0,010	0,033	0,048	0,038	0,033	9,270	4,423
6	655,36	0,001	0,020	0,010	0,035	0,039	0,037	0,036	9,127	4,971
7	764,59	0,001	0,022	0,012	0,041	0,034	0,033	0,040	9,212	4,598
8	873,32	0,013	0,013	0,014	0,055	0,028	0,057	0,045	9,326	4,041

Table 26. Concentrations through time for the 8th experiment.